Coordination Chemistry Reviews, 68 (1985) 53–99
Elsevier Science Publishers B.V., Amsterdam – Printed in The Netherlands

HYDROGENASE AND ITS APPLICATION FOR PHOTOINDUCED HYDROGEN EVOLUTION

ICHIRO OKURA

Department of Chemical Engineering, Tokyo Institute of Technology, Meguro-ku, Tokyo 152 (Japan)

(Received 3 July 1984; in revised form 10 September 1984)

CONTENTS

A. INTRODUCTION

The enzyme hydrogenase (hydrogen: oxidoreductase, EC 1.12) catalyzes the reversible oxidation of hydrogen as represented by the following equation

$$H_2 \overset{\text{hydrogenase}}{\rightleftarrows} 2\,H^+ + 2\,e^- \qquad (1)$$

Hydrogenase has been studied for some decades. The enzymes are widespread in bacteria and algae, and an increase in the range of organisms examined and an improvement in purification techniques have allowed characterization of hydrogenase from a variety of bacterial sources. The hydrogenases were identified throughout as iron–sulfur proteins. The recent observation of nickel as a constituent of hydrogenases from certain organisms is stimulating further studies of the active site of hydrogenase.

In the last half-dozen years, since the discovery of photoinduced hydrogen evolution from water by the coupling of hydrogenase and chloroplasts, research on hydrogenase has gained practical significance, since hydrogen

0010-8545/85/$16.45

TABLE 1

Properties of hydrogenase

Source	Molecular weight	Fe (mol)	Labile-S (mol)	Fe–S center	ESR absorption		References
					Oxidized	Reduced	
Chromatium	98000	4	4	–	$g > 2$	silent	4,5,6
Rhodospirillum rubrum	66000	4	4	–	$g > 2$	silent	7,8
Alcaligenes eutrophus H16	205000	12	12	$2\times[Fe_4S_4]$ $2\times[Fe_2S_2]$	$g = 2.02$	$g = 2.04, 2.00, 1.95, 1.93, 1.86$	9,10
Escherichia coli	113000	12	12		$g > 2$	$g > 2$	11
Clostridium pasteurianum	60000	12	12	$3\times[Fe_4S_4]$	$g > 2$	$g = 2.079, 1.961, 1.892$	12–14
Desulfovibrio vulgaris (Miyazaki)	89000	8	8	$2\times[Fe_4S_4]$			15–19
Desulfovibrio vulgaris (Hildenborough)	50000	12	12				20,21
Desulfovibrio gigas	89000	12	12	$3\times[Fe_4S_4]$		silent	22,23

may be considered as an ideal fuel for the future.

The aim of this review is to discuss hydrogenase catalysis and the extensive research concerning photoinduced hydrogen evolution with hydrogenase as an application of this enzyme. I describe studies of the hydrogenase from *Desulfovibrio vulgaris* (Miyazaki) and its application, made in my laboratory from 1977, combined with an unavoidably incomplete selection of data and references from the current literature. For historical details, and an extensive survey of the physiological role of hydrogenases, the reader is referred to previous reviews [1–3].

B. PROPERTIES OF HYDROGENASE

Hydrogenases obtained from bacteria or algae have been extensively purified and characterized, and extensive evaluation of the physical and chemical properties of hydrogenase has been undertaken; the properties are summarized in Table 1. This Table shows that hydrogenases characterized so far are a very peculiar group of enzymes. Hydrogenases commonly contain iron and acid-labile sulfide groups, and spectroscopically show a broad shoulder in the 400 nm region, typical of iron–sulfur proteins. For example *Clostridium pasteurianum*, *Desulfovibrio vulgaris*, and *Chromatium* hydrogenases contain 12Fe–12S, 8Fe–8S, and 4Fe–4S per enzyme molecule respectively.

Structures of the hydrogenase active sites were established by ESR analysis and core-extrusion techniques, as will be discussed later.

In this section, some characteristics of hydrogenase are outlined and some of the methods involved in the determination of these characteristics are shown.

(i) Hydrogenase active sites

Effect of inhibitors

The effect of a number of inhibitors on the hydrogen evolution activity of hydrogenase is shown in Table 2 [18]. Some of the heavy metals, e.g. mercury, copper, and silver, strongly inhibit the enzymatic activity, in spite of their low concentration compared with that of the enzyme. Mercuric chloride, especially, completely inhibits the enzymatic activity. This was also found for the hydrogenase of *Scenedesmus*, *Proteus vulgaris* [24] and *Chromatium* [25]. The degree of inhibition by heavy metals was in the same order as their ionization potentials: Hg(II) > Cu(II) > Fe(II), Fe(III), Ni(II). These data suggest that hydrogenase inhibition is caused by bonding between the inhibitor and hydrogenase or by metal exchange in the active sites.

Some chelating inhibitors had a partial inhibiting effect on the enzymatic activity, while other hydrogenases are not inhibited by *o*-phenanthroline

TABLE 2

Inhibition of hydrogenase [18]. (The enzyme (1.0×10^{-6} mol dm^{-3}) was preincubated with inhibitors for 1 day at room temperature. The activity was measured with an enzyme-inhibitor solution diluted six times.)

Inhibitor	Concentration (M)	Inhibition (%)
$HgCl_2$	5.0×10^{-5}	100
	5.0×10^{-6}	100
$CuSO_4$	5.0×10^{-5}	78
	5.0×10^{-6}	75
$AgNO_3$	5.0×10^{-5}	77
	5.0×10^{-6}	73
$NiSO_4$	6.4×10^{-6}	0
$FeSO_4$	6.4×10^{-6}	0
$Fe_2(SO_4)_3(NH_4)_2SO_4$	3.5×10^{-6}	0
Urea	5.0×10^{-1}	44
Thiourea	5.7×10^{-2}	48
o-Phenanthroline	2.5×10^{-3}	45
EDTA[a]	2.0×10^{-3}	89

[a] Two days' incubation at 4°C.

[24,25]. The fact that some chelating agents have an effect on active hydrogenase suggests that the iron is not firmly bound in the active enzyme.

The cause of the strong inhibition in the presence of mercuric chloride, even at low concentration, has been clarified by the following experiments. A mixture of hydrogenase and mercuric chloride was filtered by Diaflo PM-30 membrane and the amount of iron and its activity in both the filter cake and the filtrate were measured. The iron content of the filtrate increased the longer the hydrogenase and mercuric chloride were mixed, but no activity was observed in the filtrate. On the contrary, the iron content of the filter cake decreased. The relation between the activity of the filter cake and the amount of extracted iron per enzyme molecule is shown in Fig. 1. The activity decreased linearly with the amount of extracted iron and reached zero when the extracted iron per enzyme molecule was two. Although iron still remained in the enzyme, no activity was observed. This result indicates that two iron atoms of the eight per molecule (hydrogenase from *Desulfovibrio vulgaris* (Miyazaki) contains eight iron atoms per enzyme molecule) are easily extracted compared with the other six. It is also evident that each iron atom does not always make up a hydrogenase-active site individually. The relation between the activity of the filter cake and the number of mercury atoms remaining in hydrogenase is also shown in Fig. 1. The activity decreases linearly with the amount of mercury remaining and

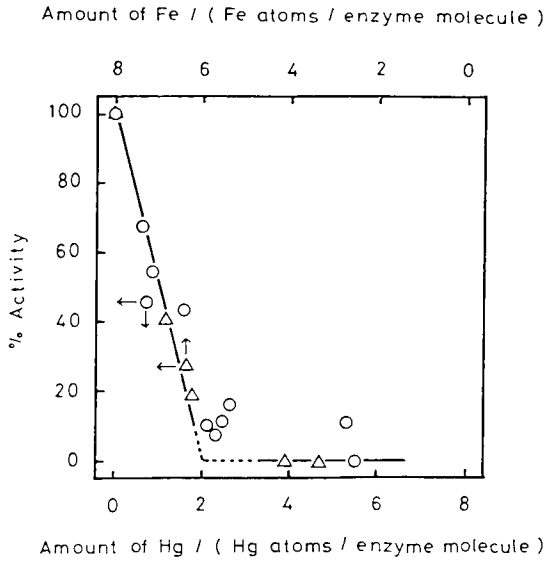

Fig. 1. Relationship between hydrogenase activity and the number of iron atoms (△) and mercury atoms (○) per enzyme molecule [18].

reaches zero when the mercury atoms per enzyme molecule are two. Although iron still remains in the enzyme, no activity is observed. This indicates that the mercury atoms are exchangeable with the iron atoms in hydrogenase, and two active sites with iron–sulfur clusters per hydrogenase molecule may be proposed similar to the iron–sulfur clusters of the type found in ferredoxins.

Nakos and Mortenson [26] found that mersalyl (a mercury derivative) inhibited *Clostridium pasteurianum* hydrogenase, suggesting that mercury ion interacts with the acid-labile sulfur and that the reaction should release iron. Indeed, it was found that metal-complexing reagents reacted with the iron present in the enzyme only after prior treatment of the enzyme with mersalyl.

The type of iron–sulfur cluster present in hydrogenase

All iron–sulfur proteins so far investigated contain one, two, three or four iron–sulfur clusters (Fig. 2). The structures of at least part of the active sites of some hydrogenases have been established by use of the core-extrusion technique. The general reaction is given by the following equation

$$Fe_xS_x(SR)_4^{2-} + 4\ R'SH \rightarrow Fe_xS_x(SR')_4^{2-} + 4\ RSH \qquad (2)$$

($x = 2$ or 3)

Under partially denaturing conditions in aqueous/aprotic solvent mixtures,

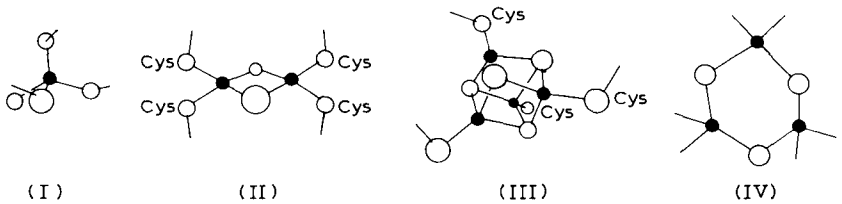

Fig. 2. Atomic arrangements in the one-iron (rubredoxin, I), two-iron (II) and four-iron (III) clusters, and the proposed three-iron cluster (IV).

the active center of iron–sulfur proteins exchanges with organic thiols, e.g., thiophenol, to give the two-iron $[Fe_2S_2(SPh)_4]^{2-}$ or four-iron $[Fe_4S_4(SPh)_4]^{2-}$ analog cluster [27,28].

When hydrogenase from *Desulfovibrio vulgaris* (Miyazaki) was dissolved in an 80% hexamethylphosphoramide: 20% water mixture, in the presence of 100-fold excess of thiophenol, the absorption of the resulting solution resembled that of the Fe_4S_4 (thiophenyl)$_4$ dianion (Fig. 3). Thus, hydrogenase contains an iron–sulfur structure that yields thiophenyl-four-iron clusters. On the other hand, two-iron clusters yield a spectrum of Fe_2S_2-(thiophenyl)$_4$ dianion (Fig. 3) which is apparently different from the hydrogenase cluster. A similar result has been reported in another hydrogenase from *Clostridium pasteurianum* [30]. The presence of an Fe_4S_4 cluster has been indicated by using hydrogenase from *Desulfovibrio gigas* which con-

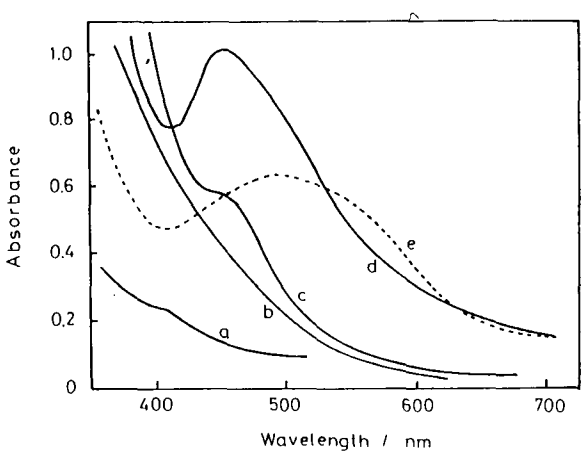

Fig. 3. Active site core extrusion of hydrogenase with RSH in 4:1 hexamethylphosphoramide (HMPA)/H_2O [18,29]. (a) absorption spectra of hydrogenase (75 μM); (b) a mixture of 1 ml of (a), 4 ml of HMPA and 0.1 ml of PhSH after 1 min mixing; (c) (b) after 1 day; (d) $[Fe_4S_4(SPh)_4]^{2-}$; (e) $[Fe_2S_2(SPh)_4]^{2-}$.

tains 12 iron atoms and 12 acid-labile sulfur groups per molecule [31]. These results also strongly suggest the presence of two Fe_4S_4 clusters per molecule of hydrogenase.

If we assume that a Fe_4S_4 cluster is the site of hydrogen activation or production, then an explanation for the function of the other cluster is needed. As Adams et al. [3] have proposed, one probable function lies in the transfer of electrons to and from the active site. Thus an external carrier such as ferredoxin or cytochrome c_3 would transfer electrons to or from these "accessory" sites and the electron would then be passed by an intramolecular mechanism to the hydrogenase site at which, when combined with protons, hydrogen is evolved.

Nickel in hydrogenase

Hydrogenases have been recognized so far to be iron–sulfur proteins, and it has been reported that no additional metal is contained. Very recently, however, it has been ascertained that nickel was essential for the catalytic activity of hydrogenase. Nickel was shown to be a structual component of the hydrogenases isolated from *Desulfovibrio gigas* [32,33], *Desulfobibril desulfuricans* (ATCC 27774) [34], *Desulfovibrio desulfuricans* (Norway 4) [35], *Methanobacterium* (strain Marburg) [36], *Methanobacterium thermoautotrophicum* (strain ΔH) [37], *Chromatium vinosum* [38] and *Alcaligenes eutrophus* [39]. With the exception of the last two, ESR nickel redox-dependent signals were reported.

Moura et al. [40] strongly suggest nickel is involved in the catalytic activity. Friedrich et al. [39] found that nickel was a constituent of the soluble and particulate hydrogenase of *Alcaligenes eutrophus*. Incorporation of $^{63}Ni^{2+}$ revealed that almost all the nickel taken up by the cells was bound to the protein. Chromatography (Fig. 4) of a crude extract on diethylaminoethyl cellulose demonstrated an association of $^{63}Ni^{2+}$ with soluble and particulate hydrogenases. This was supported by further analysis such as polyacrylamide gel electrophoresis. X-ray fluorescence analysis of the homogeneous soluble hydrogenase indicated the presence of 2 mol of nickel per mol of enzyme, whereas the amount of nickel determined by incorporation of $^{63}Ni^{2+}$ was calculated to be approximately 1 mol (mol-enzyme)$^{-1}$. Cells grown under nickel limitation contained catalytically inactive, but serologically active, soluble and particulate hydrogenase. It is concluded that nickel is essential for the catalytic activity of hydrogenase and is not simply involved as a regulatory component in the synthesis of this enzyme.

Kojima et al. [37] found tightly-bound nickel in two hydrogenases from the methanogenic bacterium *Methanobacterium thermoautrophicum* (strain ΔH) and found the anticipated iron–sulfur atoms with a fixed ratio of 15–20 iron atoms per nickel. One hydrogenase reduced the 8-hydroxy-5-deazaflavin

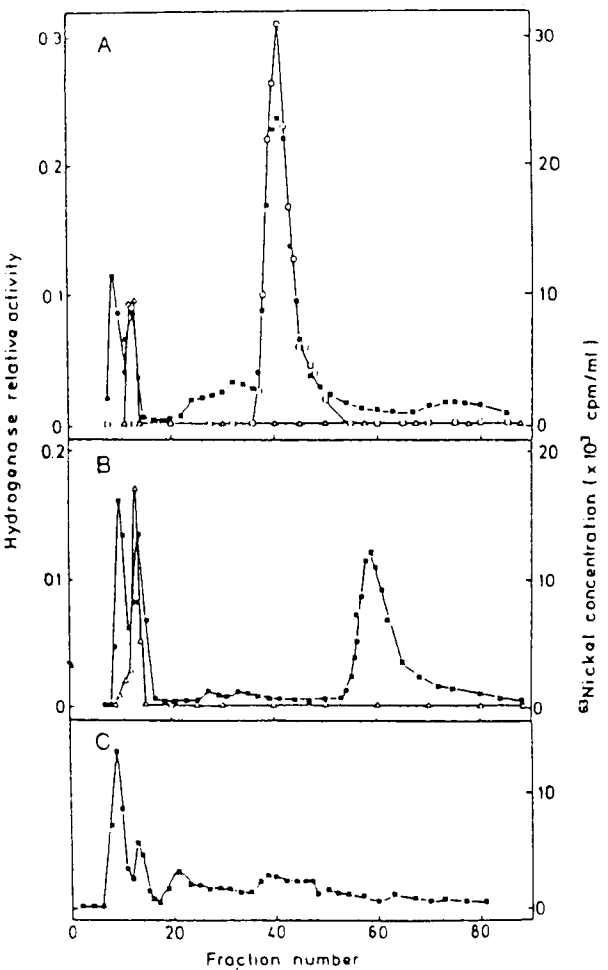

Fig. 4. Chromatography of extracts of *A. eutrophus* on DEAE-cellulose. About 3.5 ml of crude extracts from cells of strain H 16 (A), strain HF 16 (B), and strain HF 18 (C) grown in 100 ml of fructose–glycerol mineral medium in the presence of 0.07 μM $^{63}Ni^{2+}$ (0.05 μCi/ml) were subjected to chromatography on DEAE-cellulose. From the eluate fractions, 100 μl was used to determine radioactive nickel (■). For determination of the particulate hydrogenase (△), 100 μl was used, and 50 μl was used for the soluble hydrogenase activity (□). Reproduced by permission of the publisher from ref. 39.

coenzyme factor 420 (F_{420}), whereas another has been purified as a methyl-viologen-reducing hydrogenase. Both enzymes possess an ESR signal (Fig. 5) attributed to paramagnetic nickel as demonstrated by hyperfine coupling in ^{61}Ni-containing hydrogenases. Upon replacement of hydrogen by argon in the gas phase over the reduced, active F_{420}-reducing enzyme, several ESR signals appear, including two signals at $g = 2.140$ and 2.196 which reflect a

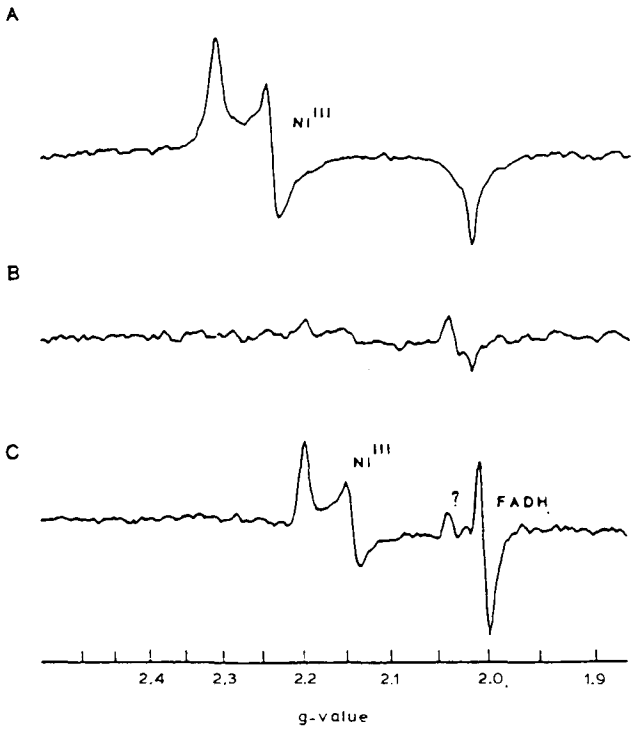

Fig. 5. ESR spectra of F_{420}-reducing ^{59}Ni-hydrogenase as isolated (spectrum A), reduced with H_2 (spectrum B), and after argon replacement of H_2 (spectrum C). The enzyme was reduced under H_2 in 1 M KCl/50 mM Tris-HCl buffer, pH 7.5, at room temperature and incubated at 45°C for 1 h. Reproduced by permission of the publisher from ref. 37.

new form of paramagnetic nickel(III), and also a signal at $g = 2.036$ which may be an iron signal. In contrast to the hydrogenase of *Clostridium pasteurianum*, which appears to use only iron–sulfur prosthetic groups and which reacts with one-electron-transfer agents, this methanogen hydrogenase seems to utilize iron, nickel, and flavin redox sites and to reduce one-electron (viologen) and two-electron (deazaflavin) oxidants.

ESR spectra attributed to different nickel valences have been observed in oxidized and reduced forms of hydrogenase from *Desulfovibrio gigas*. However, it has been reported that hydrogenase from *Desulfovibrio vulgaris* (Hildenborough) does not contain nickel [41]. Thus, the role of nickel in the activity of hydrogenase has not yet been clarified.

Reconstitution of hydrogenase from its apoprotein

A procedure has been described for the removal of iron and labile sulfide from Clostridial ferredoxin to isolate apoferredoxin, and the reconstitution of ferredoxin from this protein [42–44]. This procedure, which has consider-

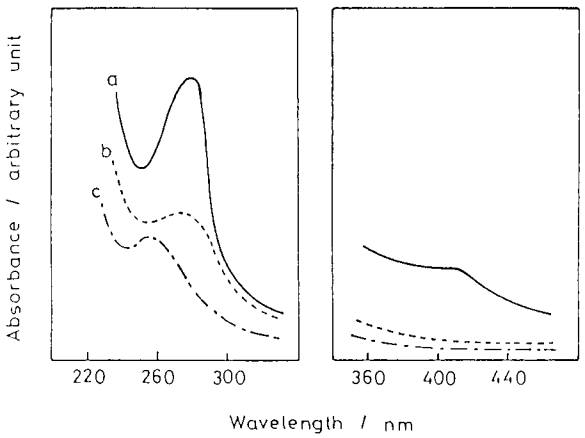

Fig. 6. Spectra of hydrogenase (a), apoprotein (b) and reconstituted hydrogenase (c) [29].

able utility, is being applied to other iron–sulfur proteins such as spinach ferredoxin [45], adrenodoxin [46], and putidaredoxin [47], and is also useful in increasing the sensitivity of the Mössbauer method by which proteins enriched in ^{57}Fe are obtained [48,49].

The hydrogenase from *Desulfovibrio vulgaris* contains two Fe_4S_4-clusters per enzyme molecule from the formation of the Fe_4S_4 $(thiophenyl)_4$ dianion by the addition of thiophenol. The method used for the preparation of apoprotein was a modification of Rabinowitz et al. [42–44] and Rao et al. [48].

Hydrogenase (1.2×10^{-8} mol) in 6.0 dm^3 of phosphate buffer was treated with 2.0 dm^3 of 20% trichloroacetic acid and flushed with nitrogen gas for 3 h to expel H_2S. The mixture was centrifuged at 20000 g for 20 min. The precipitate was washed with water, 5% trichloroacetic acid, again with water and resuspended in 4.5 dm^3 of 0.05 mol dm^{-3} Tris-HCl buffer.

The spectrum of the resulting solution is shown in Fig. 6, curve b. The solution has no absorption at 420 nm attributable to the iron–sulfur cluster, but that at 280 nm remains, and iron was not detected in this solution. This implies that the solution contains the apoprotein without an iron–sulfur cluster.

Reconstitution of hydrogenase from its apoprotein is carried out as follows. The apoprotein (4 ml) was treated with 0.2 dm^3 of 2-mercaptoethanol for 2.5 h at room temperature under nitrogen atmosphere. Sodium sulfide, 0.5 dm^3 (4×10^{-2} mol dm^{-3}), and 0.5 dm^3 of $FeCl_3$ (4×10^{-2} mol dm^{-3}) or $FeSO_4(NH_4)_2SO_4$ were added (Table 3). The reconstituted hydrogenase was separated from excess of reagent by passing through a column (1.5×15 cm) of Sephadex G-50. Reconstitution required the addition of a source of

TABLE 3

Reconstitution of hydrogenase from apohydrogenase [29]

Preparation system	Preparation condition	Activity (%)
Hydrogenase (holoprotein)	–	100
Apohydrogenase	–	0
Apohydrogenase + Na_2S	At room temp. for 1 day	0
Apohydrogenase + Fe^{2+}	At room temp. for 1 day	0
Apohydrogenase + Na_2S + Fe^{2+}	At room temp. for 1 day	0
Apohydrogenase + Na_2S + $FeCl_3$ + $HSCH_2CH_2OH$	At room temp. for 1 day	1.4
Apohydrogenase + Na_2S + $FeSO_4(NH_4)_2SO_4$ + $HSCH_2CH_2OH$	At room temp. for 1 day	1.03
Na_2S + $FeSO_4(NH_4)_2SO_4$ + $HSCH_2CH_2OH$	At room temp. for 3 hrs	0

The apoprotein (4 ml) was treated with 0.2 ml of 2-mercaptoethanol for 2.5 h at room temperature under nitrogen. Sodium sulfide, 0.5 ml (4.0×10^{-2} M), and 0.5 ml of $FeCl_3$ (4.0×10^{-2} M) or $FeSO_4(NH_4)_2SO_4$ were added. The reconstituted hydrogenase was separated from excess of reagent by passing through a column (1.5×15 cm) of Sephadex G-50.

ionic iron, inorganic sulfide, and mercaptide reducing agent. These were supplied by $FeCl_3$ or $FeSO_4(NH_4)_2SO_4$, sodium sulfide and 2-mercaptoethanol. No reconstitution was observed if any of these components were omitted. Though the activity of the reconstituted hydrogenase is very low compared with the original, the turnover number per hydrogenase molecule was 32 min^{-1} (mol-enzyme)$^{-1}$. This shows that only a small portion of the apoprotein is reconstituted. For this reason, the extinction peak at 420 nm might not be observed (Fig. 6, curve c).

(ii) Mechanism of hydrogenase catalysis

Purification of hydrogenase and assay of hydrogenase activity

Hydrogenase from *Desulfovibrio vulgaris* (Miyazaki) has been purified [19]. The particulate fraction of the bacterial sonicate was digested with trypsin at 4°C for one day under a nitrogen atmosphere. The solubilized hydrogenase was precipitated with ammonium sulfate at 70% saturation, the precipitate dissolved in water, concentrated by a Diaflo PM-30 membrane, and chromatographed on a Sephadex G-150 column (2.7×68 cm) with 0.02 mol dm^{-3} Tris-HCl (pH 7.3) containing 0.08 mol dm^{-3} NaCl as an eluting buffer. Further purification was carried out, if necessary, by a DEAE Sephadex G-50 column, which had been equilibrated with 0.05 mol dm^{-3} Tris-HCl buffer, the hydrogenase being eluted by linear concentration gradient with a mixing chamber containing 160 dm^3 of 0.01 mol dm^{-3} Tris-HCl

(pH 7.3) and a reservoir containing 160 dm^3 of 0.075 mol dm^{-3} NaCl in 0.04 mol dm^{-3} Tris-HCl.

Hydrogenase activity was assayed by measuring the rate of evolution of hydrogen from reduced methylviologen. The reaction mixture contained hydrogenase (0.5 nmol), 2.33 μmol of methylviologen, and $Na_2S_2O_4$ (5.0 mg) in 3.0 dm^3 of 0.02 mol dm^{-3} phosphate buffer. The hydrogenase activities are expressed as micromol hydrogen evolved per min.

The homogeneity of the hydrogenase obtained by this means was confirmed by isoelectric focusing and ultracentrifugation techniques. For the characterization of the enzyme such as stability and pH limitation, see ref. 19.

Kinetics of hydrogen production

The amount of hydrogen evolved increases gradually and reaches a constant value, and this value depends on the equimolar amount of $Na_2S_2O_4$ added (Fig. 7). The addition of a further, similar amount of $Na_2S_2O_4$ (20.4 mg) to the system, after cessation of the initial hydrogen evolution, results in a further evolution of hydrogen, as shown by the arrow in Fig. 7. The same amount of hydrogen was evolved; the initial evolution rate was almost the same as that of the original hydrogen evolution. This indicates that the enzyme is not deactivated during the reaction. From the stoichiometry of the reaction, the following equation is proposed.

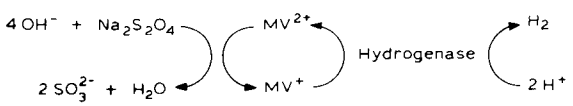

(3)

$$S_2O_4^{2-} + 4\,OH^- + 2\,H^+ \longrightarrow 2\,SO_3^{2-} + 2\,H_2O + H_2$$

It was confirmed that hydrogen was produced from protons in water by using D_2O instead of H_2O.

At the low concentration of $Na_2S_2O_4$, the initial rate does not depend on the concentration, but at the higher concentration the rate decreases as the concentration increases. Since the pH of the solution decreases at the higher concentration, the rate decrease may be caused by the pH change. Hydrogenase is easily reduced in the presence of $Na_2S_2O_4$, but no hydrogen evolution is observed from the hydrogenase so reduced. Hydrogenase cannot simply store electrons for hydrogen evolution, but needs suitable electron transfer reagents for proton reduction to form hydrogen. The initial rate increases with methylviologen concentration at all temperatures examined. As methylviologen is a one-electron transfer reagent, two molecules of methylviologen are needed for the production of one molecule of hydrogen.

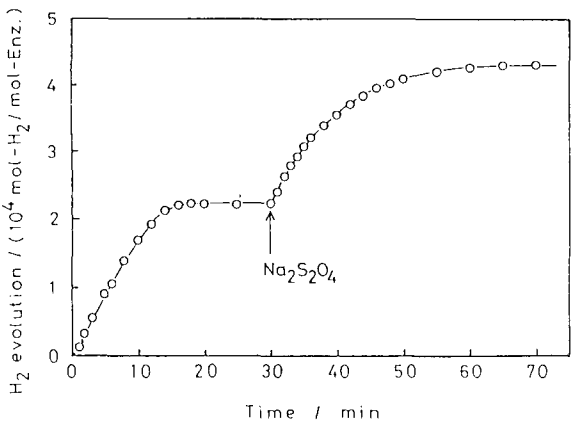

Fig. 7. Time dependence of hydrogen evolution from reduced methylviologen catalyzed by hydrogenase [18]. Methylviologen, 7.57×10^{-4} M; $Na_2S_2O_4$, 20.4 mg; hydrogenase, 2.4×10^{-7} M. Total volume, 12 ml; pH, 7.0.

Consequently, the following hydrogen evolution mechanism is considered

$$E + S \overset{K}{\rightleftarrows} ES$$

$$ES + S \overset{K'}{\rightleftarrows} ES_2 \tag{4}$$

$$ES_2 + 2\,H^+ \overset{k}{\rightarrow} E + 2\,S_{ox} + H_2$$

where E is an enzyme, and S and S_{ox} are the reduced and oxidized forms of the substrate, respectively. K and K' are the equilibrium constants and k is the rate constant. On the basis of this mechanism, the hydrogen evolution rate, V, is expressed as follows

$$V = kKK'[S]^2/(1 + 2K[S] + KK'[S]^2)$$

If it is assumed that $K = K'$, the equation is simplified

$$V = kK^2[S]^2/(1 + K[S])^2 \tag{5}$$

or

$$\frac{[S]}{V^{1/2}} = \frac{[S]}{k^{1/2}} + \frac{1}{k^{1/2}K} \tag{6}$$

A plot of $[S]/V^{1/2}$ vs. [S] is shown in Fig. 8(a). Good linear relationships were obtained at each temperature, which supports the mechanism above and also shows that the equilibrium constants in eqn. (4) must be similar. A plot of $[S]/V$ vs. [S] was also tried but there were deviations (Fig. 8(b)).

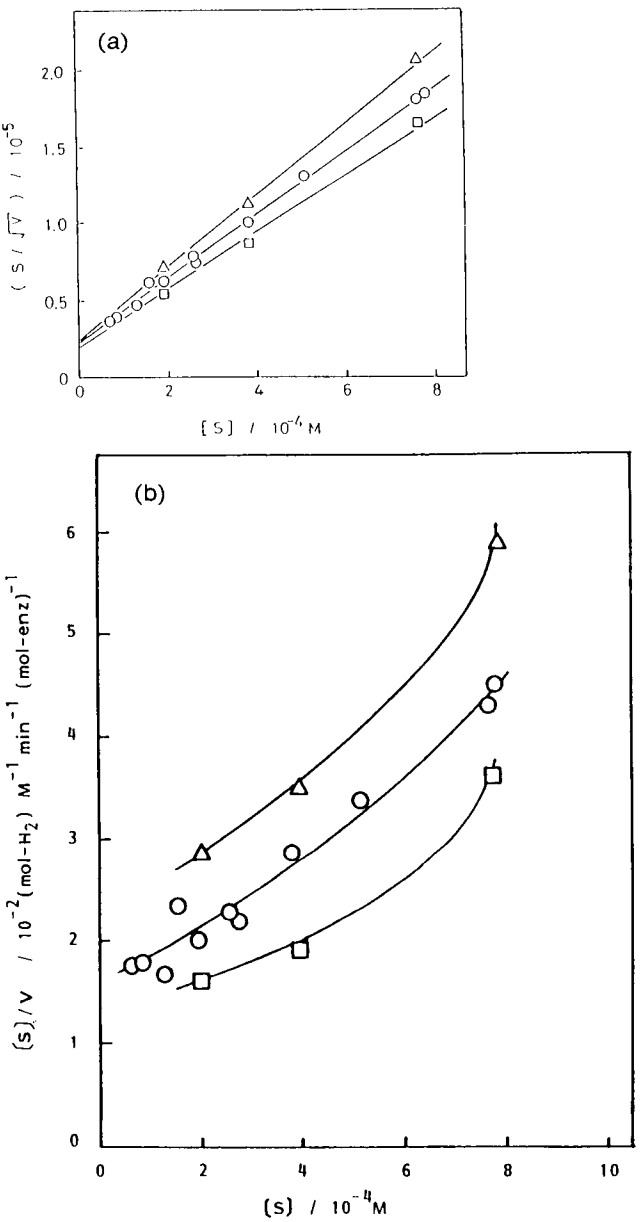

Fig. 8. (a) Rate (V) of hydrogen evolution from reduced methylviologen ([S]) catalyzed by hydrogenase [18]. Relationship between $[S]/V^{1/2}$ and [S] at 25°C (△), 30°C (○) and 35°C (□). (b) Relationship between $[S]/V$ and [S] at 25°C (△), 30°C (○) and 35°C (□).

From the slopes and the intercepts in Fig. 8(a), values of k (turnover number), K, and the activation parameters for hydrogen evolution were calculated; $K = 8.8 \times 10^3$ mol^{-1} dm^3, $k = 2.3 \times 10^{-3}$ min^{-1} (enz-

molecule)$^{-1}$ at 30°C, $E_K = 0$ kJ mol^{-1}, $E_k = 8$ kJ mol^{-1}. Chen and Mortenson [50], Erbes and Burris [51] and Glick et al. [52] obtained linear plots of $1/V$ vs. $1/[S]$ (where S is hydrogen or methylviologen) but high concentrations of the reduced carriers, conditions under which van Dijk et al. [53] obtained maximum non-linearity, were not examined. High concentrations of methylviologen were avoided by some because of the complications caused by stronger binding of the dimer to hydrogenase. The double reciprocal plots indicate that hydrogen and methylviologen bind sequentially in the hydrogen oxidation reaction, but the results do not distinguish between an ordered or random sequence. A reaction between a carrier reduced by $Na_2S_2O_4$ and a proton does not fit the data of van Dijk et al. [53]. Since the plots are linear when the one-electron carrier, methylviologen, is used it can be concluded that only one methylviologen reacts at a time and there is no cooperation.

Kinetics of methylviologen reduction by hydrogen catalyzed by hydrogenase

Many types of electron acceptors which can be reduced by hydrogen have been found as hydrogenase substrates. The reaction mechanism for reduction of methylviologen with hydrogenase may be discussed on the basis of the kinetic data.

When a solution containing hydrogenase and methylviologen was stirred under a hydrogen atmosphere, formation of the methylviologen cation radical, MV^+, was observed. MV^+ concentration increased gradually with

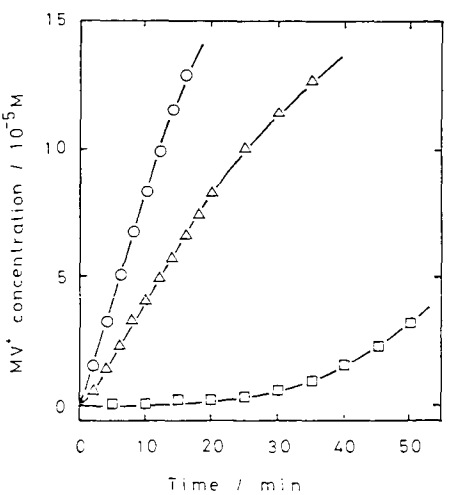

Fig. 9. Time dependence of MV^+ production catalyzed by hydrogenase under hydrogen atmosphere. Reaction conditions: MV^{2+}, 1.29×10^{-3} M, $P_{H_2} = 106$ Torr; hydrogenase, ○: 4.22×10^{-9} M, △: 2.11×10^{-9} M, □: 4.22×10^{-9} M (hydrogenase is not activated). pH, 7.0. Reproduced by permission of the publisher from ref. 54.

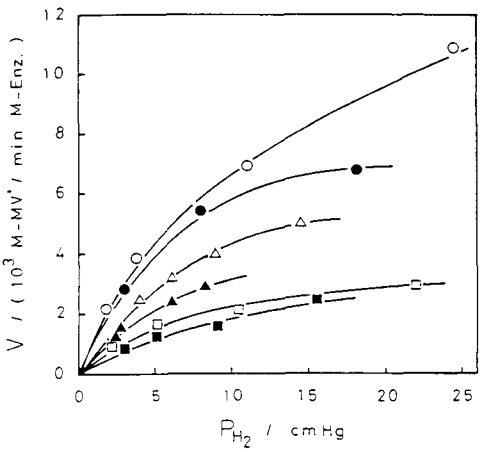

Fig. 10. Rate of MV^+ production catalyzed by hydrogenase under hydrogen atmosphere. The dependence of MV^+ production rate on hydrogen pressure. ○, 63.0 mM; ●, 42.0 mM; △, 5.03 mM; ▲ 2.52 mM; □, 1.29 mM; ■, 0.968 mM. pH, 7.0. Reproduced by permission of the publisher from ref. 54.

time after a long induction period (Fig. 9, curve c). The induction period may be required for activation of hydrogenase by hydrogen. As it is known that dithionite can reactivate hydrogenase that has been exposed to air, dithionite-treated hydrogenase was also studied. When the dithionite-treated hydrogenase (final concentration 0.7×10^{-3} mol dm^{-3}) was used, no induction period was observed and the MV^+ concentration increased linearly with time at the initial stage of the reaction (Fig. 10, curves a and b as typical examples). Only the treated hydrogenase had no reduction ability for methylviologen without hydrogen, after removal of the dithionite with air.

Initial rates were obtained from the slope of the linear part of the curves at the initial state of the time course. The initial rate of MV^+ formation, V, was proportional to the amount of hydrogenase and was dependent on the hydrogen pressure (Fig. 10). The rates increase with hydrogen pressure and reach constant values which seem to be dependent on methylviologen concentration. The double reciprocal plots for methylviologen reduction are shown in Fig. 11 in which each line extrapolates to the same point. Thus, it is necessary for methylviologen to combine with hydrogenase before hydrogen desorbs as a proton bonded with hydrogenase, i.e. this is a sequential mechanism. If the reaction proceeded by a "ping-pong" mechanism, in which methylviologen combines with hydrogenase after the desorption of a proton, all of the lines would be parallel.

Since each line extrapolates to a single point on the abscissa, hydrogen and methylviologen do not combine with hydrogenase in a regular order, i.e. a random mechanism is proposed. If the combination followed a regular

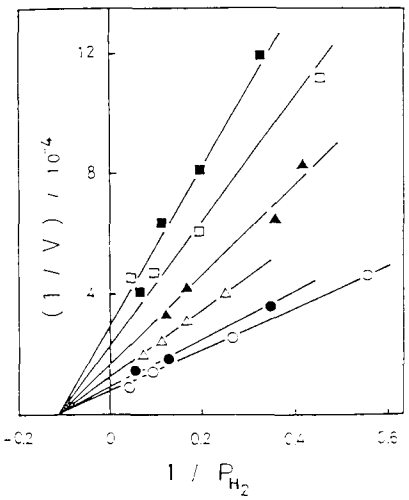

Fig. 11. Rate of MV^+ production catalyzed by hydrogenase under hydrogen atmosphere. Double reciprocal plots for MV^+ production at various hydrogen pressures. Reproduced by permission of the publisher from ref. 54.

order the point of intersection would not be on the abscissa. The value of the intersection point on the abscissa, i.e. the Michaelis constant, is independent of methylviologen concentration. Hence, the binding of hydrogen and methylviologen to hydrogenase do not interact with each other. From the above results, the following reaction mechanism is proposed

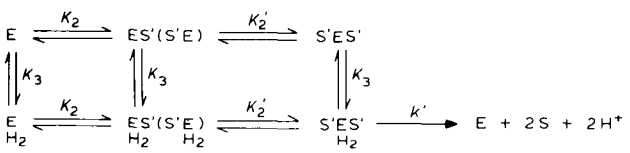

where E, S′ and S are hydrogenase, methylviologen and MV^+, respectively and $K_2 = K_2'$.

In this reaction mechanism, hydrogen and methylviologen combine with hydrogenase independently and an intermediate, H_2ES_2', is formed, followed by the formation of proton and MV^+. The reaction rate is determined by the last step.

The following rate equation is derived according to the above reaction mechanism:

$$V = (\mathrm{d}[MV^+]/\mathrm{d}t)[E]_0 = 2k'K_3K_2^2[H_2][S']^2/(1 + K_3[H_2])(1 + K_2[S'])^2 \quad (7)$$

or

$$1/V = \left((1 + K_2[S'])^2/2k'K_2^2[S']^2\right)(1 + (1/K_3[H_2])) \quad (8)$$

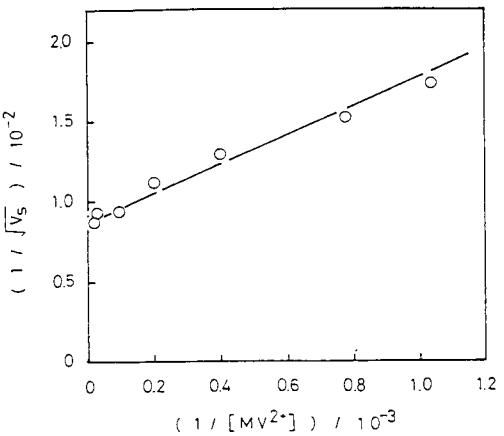

Fig. 12. Rate of MV^+ production catalyzed by hydrogenase under hydrogen atmosphere. Relationship between $1/\sqrt{V_s}$ and $1/[MV^{2+}]$. Reproduced by permission of the publisher from ref. 54.

This equation explains fully the results showing that $1/V$ was proportional to $1/[H_2]$, and that the $1/[H_2]$ values when $1/V$ was zero did not depend on the concentration of methylviologen (Fig. 11).

When the hydrogen pressure is large enough, the rate will be expressed by eqn. (9).

$$V_s = 2k'K_2^2[S']^2/(1 + K_2[S'])^2 \tag{9}$$

V_s is estimated from the intercepts of the straight lines and the ordinate in Fig. 11. Equation (9) is rewritten as

$$1/V_s = (1/2k_1)(1 + (1/K_2[S'])) \tag{10}$$

This relationship was deduced from the linearity between $1/V_s$ and $1/[MV^+]$ (Fig. 12). From Figs. 11 and 12, the rate constants are calculated: $K_2 = 1.1 \times 10^3$ mol^{-1} dm^3, $K_3 = 1.1 \times 10^4$ mol^{-1} dm^3, $k' = 6.76 \times 10^3$ min^{-1}.

The reaction mechanism for methylviologen reduction and the mechanism for hydrogen evolution from MV^+ are summarized as follows

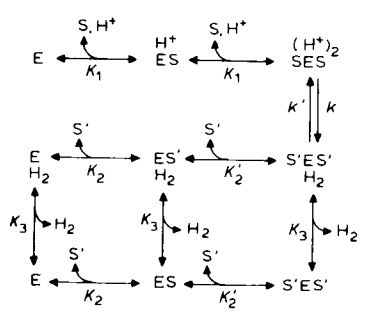

In this mechanism electron acceptors combine with hydrogenase in two rapid steps.

Erbes et al. [51] have proposed a "ping-pong" mechanism for the hydrogenase from *Clostridium pasteurianum*, in which the hydrogenase does not combine with two electron acceptors at the same time. This conclusion was derived from the fact that each line in plots of $1/V$ vs. $1/[H_2]$ intersect at a certain point, but the point is not on the abscissa.

Since our results were not consistent with a "ping-pong" mechanism, we proposed a random mechanism. Of course, the reduction of methylviologen with different hydrogenases may proceed via different mechanisms.

Yagi [19] and Erbes et al. [51] have reported that the rates of hydrogen production from MV^+ exhibit almost no isotope effect, using D_2O or D_2 instead of H_2O or H_2, indicating that protons or hydrogen are not involved in the rate-determining step. However, the rate depends strongly on the type of electron acceptors, e.g. $k = 2.3 \times 10^3$ min^{-1} for methylviologen but 2.5×10^2 min^{-1} for cytochrome c_3. Thus, the electron acceptors will be involved in the rate-determining step.

Effect of electron acceptors on hydrogenase activity

The effect of a number of additives on the hydrogen evolution activity of hydrogenase from *Desulfovibrio vulgaris* (Miyazaki) has been studied extensively [5,16,55,56,58]. All additives studied so far were known to act as inhibitors, although the extent of inhibition depended on the type of additive. When flavin mononucleotide (FMN) or methylene blue is used as

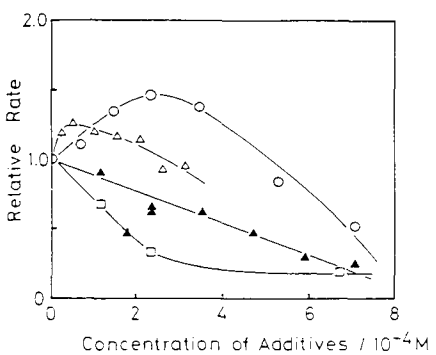

Fig. 13. Effect of additives on hydrogen evolution from reduced methylviologen catalyzed by hydrogenase [57]. The relationship between relative rates and concentration of additives. Reaction mixture contains hydrogenase (or colloidal platinum (▲)), methylviologen, $Na_2S_2O_4$ in 3.0 ml of phosphate buffer (0.02 M, pH 7.0). Additives: FMN (○, ▲); methylene blue (△); acriflavin (□). pH, 7.0.

an additive, abnormal kinetic behavior is observed. The activity increases and then decreases with FMN concentration through a maximum point (Fig. 13, curve a). A similar effect is observed with methylene blue instead of FMN (Fig. 13, curve b). When acriflavin is used, no activation is observed (Fig. 13, curve c). Though colloidal platinum can be used in place of hydrogenase, as a catalyst for hydrogen evolution from reduced methylviologen, the addition of FMN caused monotonous decrease of catalytic activity (Fig. 13, curve d). Thus, the abnormal phenomenon of the rate increase may be specific for the combination of hydrogenase and FMN or methylene blue.

In addition, it was observed that the activity of a combination of ferredoxin and methylviologen was more than the sum of the individual activities at a fixed ferredoxin concentration of 157 μmol dm^{-3} and methylviologen concentrations of less than 4 mmol dm^{-3} in the case of hydrogenase from *Clostridium pasteurianum* [3]. It was also found that cytochrome c_3 stimulated hydrogen evolution from reduced methylviologen in the *Desulfovibrio vulgaris* (Miyazaki) system [19]. This phenomenon may be explained by the following mechanism [56,58] based on the activation of hydrogen evolution from reduced methylviologen by adding cytochrome c_3

$$E + S \overset{K}{\rightleftharpoons} ES \quad ES + S' \overset{K'}{\rightleftharpoons} ESS'$$

$$E + S' \overset{K'}{\rightleftharpoons} ES' \quad ES' + S \overset{K}{\rightleftharpoons} ESS'$$

$$ES + S \overset{K}{\rightleftharpoons} ES_2 \quad ES' + S' \overset{K'}{\mapsto} ES_2'$$

$$ES_2 + 2H^+ \overset{k}{\rightarrow} E + 2P + H_2$$

$$ES_2' + 2H^+ \overset{k'}{\rightarrow} E + 2P' + H_2$$

$$ESS' + 2H^+ \overset{k''}{\rightarrow} E + P + P' + H_2$$

where E is hydrogenase, S and P are reduced and oxidized forms of methylviologen, and S′ and P′ are reduced and oxidized forms of FMN, respectively. K, K', k and k'' are kinetic constants. This mechanism is based on the assumption that two coordination sites per enzyme exist and both electron acceptors can coordinate at the same sites competitively. As FMN cannot be an electron acceptor by itself [55], k' should be zero. The rate, V, is expressed in eqn. 11

$$V = \left(kK^2[S]^2 + k'K'^2[S']^2 + 2k''KK'[S][S']\right)/(1 + K[S] + K'[S'])^2 \qquad (11)$$

According to this equation, when $k' = 0$ and [S] = constant, V should increase and then decrease through a maximum point with FMN concentration, and the abnormal observation is explained kinetically. The results above show that methylviologen and FMN can coordinate at the same site on the enzyme. The rate when methylviologen and FMN occupy two different coordination sites, is larger than that when methylviologen occupies both sites.

Effect of flavins on D_2–H_2O exchange reactions with hydrogenase

The reaction of hydrogen with hydrogenase in the absence of electron carriers was proposed in eqn. 12

$$H_2 + E \rightarrow EH^- + H^+ \text{ (where E is hydrogenase)} \qquad (12)$$

This heterolytic splitting of the hydrogen molecule was deduced by following H and D in experiments where the enzyme catalyzed exchange in the presence of D_2 and H_2O or H_2 and D_2O. From this reaction, it would be expected that if it was performed in D_2O, H^+ would equilibrate rapidly with a large pool of D_2^+ and the back reaction would yield HD. When sufficient HD accumulated, the production of D_2 would be detected. In support of this, HD did not appear preferentially but D_2 was produced initially. On the other hand, in the case of hydrogenase from *Desulfovibrio vulgaris* (Miyazaki), H_2 is produced at significant rates in the initial stage of the reaction (Fig. 14). When FMN is added to the system, no change in the exchange rate is observed. This is in contrast to the hydrogen evolution reaction of methylviologen where remarkable effects from the addition of FMN are observed.

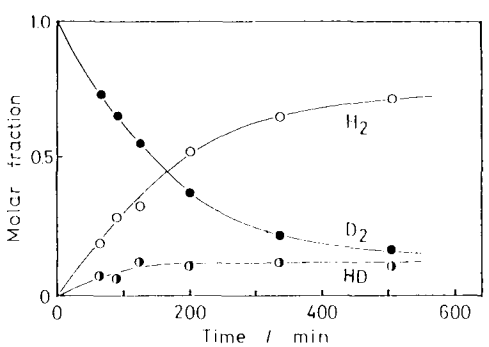

Fig. 14. Time dependence of H_2, HD and D_2 molar fractions in the D_2–H_2O exchange reaction at 30°C. The reaction mixture contains hydrogenase, $Na_2S_2O_4$, and the gas phase is D_2 at 67.5 ± 2 torr. pH, 7.0.

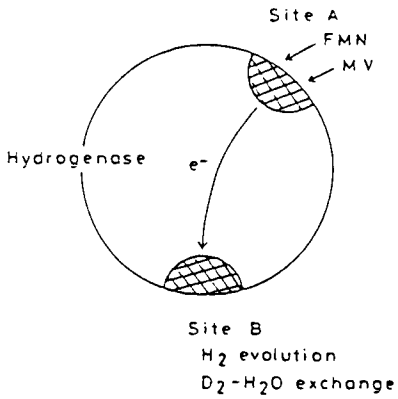

Fig. 15. Proposed active sites of hydrogenase for hydrogen evolution and D_2-H_2O exchange reactions.

When acriflavin is added to the exchange system, the activity decreases with the concentration of acriflavin.

As methylviologen and FMN are one-electron transfer reagents, two molecules of electron donor and two protons are needed for the production of one molecule of hydrogen, as shown in the earlier reaction scheme. Four molecule combinations may be difficult at the single site; two separate sites are considered (Fig. 15). A is the coordination site of electron donors where two donors can coordinate at the same time. B is the site for the D_2-H_2O exchange reaction. For hydrogen evolution both sites A and B are needed, and the electrons donated at site A can transfer easily to activate site B. Since the D_2-H_2O exchange reaction is not affected by the addition of FMN but the H_2 evolution reaction using methylviologen is affected to a remarkable degree, FMN must have a selective effect on the coordination sites of electron donors such as reduced methylviologen (site A). As acriflavin inhibits both reactions, it may coordinate to site B to inhibit not only hydrogen evolution but also the D_2-H_2O exchange reaction.

(iii) Chemical models for hydrogenase

Model studies are often of great use for the elucidation of the mechanism of enzymatic reactions. In order to elucidate the mechanism of molecular hydrogen activation by hydrogenase, a number of model studies have been carried out. To date, however, no satisfactory model systems for hydrogenase have been described.

Schrauzer et al. [59,60] reported that a system containing Fe^{2+}, S^{2-} and RS^- in the molar ratio 1:2:6 releases hydrogen efficiently, and that

hydrogen evolves from a mildly alkaline suspension of $Fe(OH)_2$. In each system, however, the iron complex is not considered to be a catalyst. Henrici-Olive and S. Olive [61] reported that Pd-SALEN (*N,N'*-ethylene-bis(salicylideneiminato)Pd(II)) activates molecular hydrogen thus catalyzing the H–D exchange and the hydrogenation of olefins. Chepaikin and Khidekel [62] also reported that Rh-ISA (rhodium(III) complexes with indigosulphonic acid) and Pt-PAN (platinum(II) complexes with 1-phenyl-azo-2-naphthol) catalyze the hydrogenation of nitroaromatics. The systems above are unsuitable as hydrogenase models, since the central metals of these catalysts are quite different from that of hydrogenase.

An artificial iron–sulfur protein has been synthesized [63,64] from bovine serum albumin (BSA) in the presence of iron, inorganic sulfide and 2-mercaptoethanol. Recently, we have found [65] that the BSA-coordinated Fe_4S_4-cluster (abbreviated as BSA-cluster) could catalyze hydrogen evolution.

In this section, the development of a hydrogen evolution system with the BSA-cluster as a hydrogenase model is described, and some physical and chemical characteristics of the BSA-cluster as an artificial hydrogenase are compared with those of the hydrogenases, and the efficacy of the cluster as a hydrogenase model is discussed.

Hydrogen evolution catalyzed by Fe_4S_4-albumin as a hydrogenase model

Holm et al. [14,27,67–73] reported the synthesis of the tetranuclear cluster complexes $[Fe_4S_4(SR)_4]^{2-}$ and binuclear cluster complexes $[Fe_2S_2(SR)_4]^{2-}$ (R = alkyl or aryl), whose structure and properties show them to be a close representation of the central cores of iron–sulfur proteins. Rabinovitz et al. [43,44] have applied Holm's core extrusion method to the preparation and isolation of the apoprotein of ferredoxin from *Clostridium pasteurianum*, and have reconstituted ferredoxin by the addition of iron(III) ions, sodium sulfide, and 2-mercaptoethanol. This procedure, which has considerable utility, is now being applied to other iron–sulfur proteins [47,74,75].

Recently we have found [16–18,29], by using the extrusion and reconstitution techniques mentioned above, that the hydrogenase from *Desulfovibrio vulgaris* (Miyazaki) contained two Fe_4S_4-type clusters per enzyme molecule. We also found two active sites per enzyme molecule by kinetics and an inhibition method with mercury(II) chloride [16,18]. The presence of these Fe_4S_4-type clusters has been established in the case of hydrogenases from *Desulfovibrio gigas* [31] and *Clostridium pasteurianum* [14]. Generally, hydrogenase is regarded as an iron–sulfur protein with Fe_4S_4-type clusters. Although the Fe_4S_4-cluster above does not have hydrogenase activity [76], the Fe_4S_4-clusters synthesized in the presence of apohydrogenase do have catalytic activity [29]. Therefore, the Fe_4S_4-cluster and also the environment of

the Fe_4S_4-cluster within a protein such as apohydrogenase, play important roles in the hydrogenase activity.

In the following section we describe the development of a hydrogen-evolution system which combines the Fe_4S_4-cluster and some protein, and compare the characteristics of the artificial and natural hydrogenase.

Preparation and properties of bovine serum albumin coordinated iron-sulfur cluster

The method used for the preparation of the albumin cluster was a modification of those of Suzuki and Kimura [63] and Lovenberg and McCarthy [64]. The preparation was carried out under a nitrogen atmosphere as follows: 80 mg of albumin was dissolved in 6 dm^3 of water containing 6.7 mmol dm^{-3} iron(II) chloride or ammonium iron(II) sulfate. 2-Mercaptoethanol (0.4 dm^3) was then added, followed by 2 dm^3 of aqueous Na_2S (0.02 mol dm^{-3}). In order to separate the albumin-cluster from excess reagent, the solution containing the albumin-cluster was placed on a Sephadex G-50 column (5 × 23 cm) with 0.02 mol dm^{-3} Tris-HCl (pH 7.0) containing 0.08 mol dm^{-3} NaCl as an eluting buffer. The eluting solution was monitored by means of the protein iron–sulfur cluster absorption bands; the results are shown in Fig. 16. Albumin was eluted at peak A. The

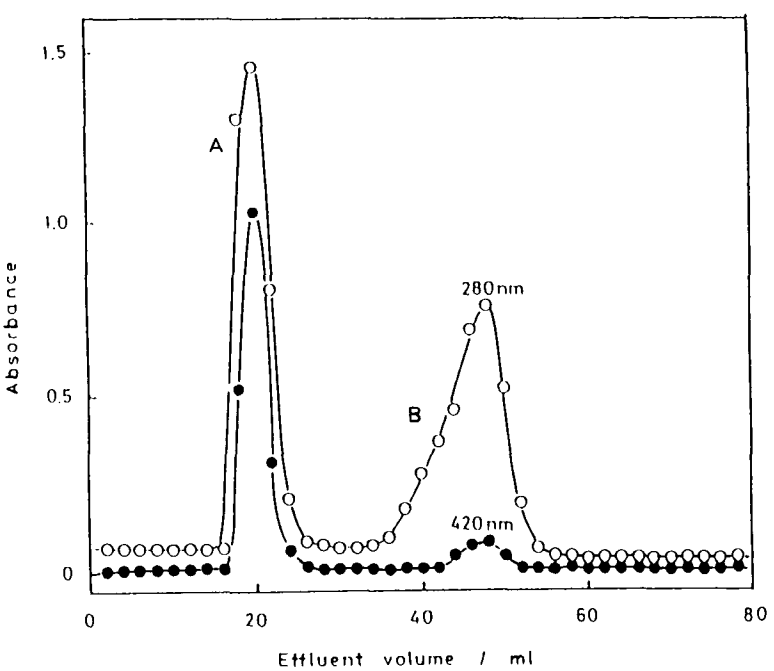

Fig. 16. Elution patterns of the BSA-cluster from a Sephadex G-50 column.

eluting solution has an absorption band at 420 nm which is attributable to the iron–sulfur clusters, but also has a molecular weight corresponding to albumin; the product is therefore not a crude mixture of albumin and the iron–sulfur cluster, but an iron–sulfur cluster incorporated in albumin. The solution was dark brown; iron(II) sulfide, formed as a by-product, may also be incorporated in the protein. Although the eluting solution corresponding to peak A was centrifuged at 20000 g for 60 min to remove the black precipitate, it was not separated from the protein completely. Iron–sulfide clusters incorporated in albumin could not be synthesized from the reaction of performed iron–sulfur cluster and albumin. Therefore, the iron(II) sulfur concomitant in the iron–sulfur incorporated in the albumin could not be avoided by this method. The specific absorption coefficients, 35600 M^{-1} cm^{-1}, at 280 nm and 14000 M^{-1} cm^{-1} at 420 nm [63], were used to estimate the concentration of protein and iron–sulfur clusters respectively. The peak B has ultraviolet and visible absorption bands which seem to be due to an excess of the 2-mercaptoethanol reagent and the synthesized $Fe_4S_4(S\text{-}CH_2CH_2OH)_4$ dianion respectively.

When the solution of iron–sulfur cluster incorporated in albumin (albumin-cluster) was incubated under a hydrogen atmosphere at 30°C, the spectrum of the solution changed. When exposed in air, the spectrum returned to its original form. A similar spectrum change has been observed in the reduction of hydrogenase from *Desulfovibrio vulgaris* by hydrogen. When excess 2-mercaptoethanol is added to the albumin-cluster solution for the identification of the core types, the absorption spectrum obtained ($\lambda_{max} = 410$ nm) resembled that of the synthesized $Fe_4S_4(S\text{-}CH_2CH_2OH)_4$ dianion (see Fig. 20, curve c). Thus the iron–sulfur clusters incorporated in albumin seem to be of the Fe_4S_4 type, but the possibility still remains that Fe_2S_2-clusters were rapidly converted to the Fe_4S_4-clusters.

Synthesis of various iron–sulfur clusters

The method used for the preparation of a series of iron–sulfur clusters with various mercapto ligands was the same as that used for the albumin-clusters. Though a number of Fe_4S_4 cores are synthesized in the presence of some thiols, SH-containing polymer, and natural proteins containing cysteinyl residues instead of apohydrogenase, an estimation has not been made whether each product is a crude mixture of protein and the iron–sulfur cluster or the iron–sulfur cluster incorporated in a compound as a ligand. No cluster complex other than the albumin-coordinated Fe_4S_4-cluster can catalyze hydrogen evolution from reduced methylviologen. Note however that the activity is lower than that of the actual enzyme, hydrogenase.

Specificity of electron carriers and kinetics

When the albumin-cluster was added to a solution of dithionite-reduced

TABLE 4

Electron carrier specificity for H_2 evolution by hydrogenase and the BSA-cluster [66]

Electron carrier	E_0' (mV)	Concentration (M)	Activity [a]	
			Hydrogenase	BSA-cluster
Cytochrome c_3	−270	5.94×10^{-7}	79	0
Flavin mononucleotide	−190	2.45×10^{-4}	trace	0
Nicotinamideadenine dinucleotide	−320	1.61×10^{-4}	4.2	4.54×10^{-3}
Coenzyme II	−324	1.72×10^{-4}	0	0
Methyl viologen	−440	2.48×10^{-4}	570	9.62×10^{-3}
Methylene blue	+11	1.96×10^{-4}	0	0
Neutral red	−325	2.03×10^{-4}	15	0
Safranine T	−289	2.07×10^{-4}	13	0
Phenosafranine	−252	1.91×10^{-4}	11	trace
Potassium ferricyanide	+360	2.01×10^{-4}	0	0

[a] Activity: (mol-H_2/min mol-cluster)

methylviologen, hydrogen was evolved under the same conditions of the hydrogenase-activity measurement. Various redox carriers were tested to see if they would replace methylviologen and mediate the electron transfer to the albumin-cluster from dithionite. The electron carrier specificities for albumin-cluster and hydrogenases are compared in Table 4. The albumin-cluster was specific for methylviologen and nicotinamideadenine dinucleotide.

The time course showed that the amount of hydrogen evolved from reduced methylviologen increased linearly with time. It is reasonable to assume that the iron–sulfur cluster in the albumin cluster (which has not been separated from iron(II) sulfide) has a central role in hydrogen evolution, because it has been confirmed experimentally that iron(II) sulfide has no activity for hydrogen evolution. With a reaction time of 44 h, the molar ratio (the turnover number) of the evolved hydrogen for the iron–sulfur cluster was 18 [65]. This means that the albumin-cluster behaves as a catalyst. Though the low term stability of the albumin cluster was not examined, it was still intact after a reaction time of 44 h.

The initial rate of hydrogen evolution increased with the methylviologen concentration until it reached a constant value. In the case of hydrogenase, the rate of hydrogen evolution from reduced methylviologen was expressed as follows [18,58]

$$V = kK^2[S]^2/(1 + K[S])^2 \tag{13}$$

or

$$[S]/V^{1/2} = [S]/k^{1/2} + 1/k^{1/2}K \tag{14}$$

where k and K are constants and where [S] is the concentration of

methylviologen. In the case of the albumin-cluster, a good linear relationship was obtained between $[S]/V^{1/2}$ and [S] (Fig. 8(a)). The plot of $[S]/V$ vs. [S] (Fig. 8(b)) for first order kinetics was also tried, but was not linear. The albumin-cluster may also catalyze hydrogen evolution by the same mechanism as that of the hydrogenase. From the slope and intercept, the equilibrium constant, K, and the rate constant, k, for hydrogen evolution from reduced methylviologen at 30°C were calculated, giving values as listed below.

Catalyst	K (M^{-1})	k (min^{-1})
Hydrogenase	8.8×10^{3}	2.3×10^{3}
Albumin-cluster	1.9×10^{4}	1.5×10^{-2}

Judging from the K values, the affinity of the albumin-cluster for methylviologen seems to be similar to that of hydrogenase. The k value for hydrogenase, however, was 10^5 times greater than that of the albumin-cluster.

C. APPLICATION OF HYDROGENASE FOR PHOTOINDUCED HYDROGEN EVOLUTION

(i) Photoinduced hydrogen evolution in the presence of electron-donating agents

Over the past few years, much attention has been given to systems capable of using solar energy. The most attractive reaction to convert solar energy into chemical energy is the photodecomposition of water into hydrogen and oxygen. Various attempts have been made to develop suitable redox systems for the photochemical utilization of solar energy. Recent work has shown that the following three component systems containing a photosensitizer, an electron donor, and an electron acceptor can be used to evolve hydrogen when a suitable catalyst is present [77–79]

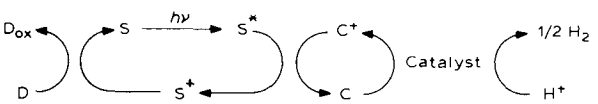

(15)

where D, S, and C are an electron donor, a photosensitizer, and an electron carrier, respectively.

The reactions described are quite general and have been demonstrated for a wide range of photosensitizers and electron carriers. Many of these are collected in Table 5. For a catalyst, an enzyme, hydrogenase, or colloidal platinum is widely used, for any of these can catalyze the reduction of protons in the presence of suitable electron donating agents such as reduced methylviologen.

TABLE 5

Various systems for photo-induced hydrogen evolution from water

Photosensitizer	Donor	Carrier	Catalyst	References
$Ru(bpy)_3^{2+}$	EDTA	MV^{2+}	Pt	84–91
$Ru(bpy)_3^{2+}$	TEA	MV^{2+}	Hydrogenase	92
			Pt	93
$Ru(bpy)_3^{2+}$	Cysteine	MV^{2+}	PtO_2	94,95
Zn-TPP $Zn\text{-}TPPS_3$	RSH	MV^{2+}	Hydrogenase	96–101
$Zn\text{-}TPPS_4$	Ascorbate	Various Viologens	Pt	102
$Zn\text{-}TPPS_4$ Zn-TMPyP	EDTA	MV^{2+}	Pt	103–106
$Cr(bpy)_3^{3+}$	EDTA	–	Pt	107
Proflavin	EDTA	MV^{2+}	Pt	108,109
Chlorophyll	Cysteine	MV^{2+}	Pt	110,111
	Ascorbate Glucose	Ferredoxin	Hydrogenase	112,113

The efficiency of the hydrogen evolution or the photoreduction of electron carrier depends on the nature of the components: a photosensitizer, an electron donor, and a catalyst. Some properties of these components used in the photoinduced hydrogen evolution system are summarized as follows.

Electron donors

Irradiation of the sample solution containing only a photosensitizer and electron carrier does not lead to accumulation of the reduced electron carrier, since the back reaction takes place very rapidly. By adding a suitable electron donor to this system, accumulation of the reduced electron carrier can often be observed. These reactions are shown as eqn. (16) when methylviologen is used as an electron carrier.

$$D + MV^{2+} \xrightarrow{h\nu} D_{ox} + MV^{+} \tag{16}$$

In this reaction, the light energy is stored in the form of chemical potential as far as the change of Gibbs's free energy (ΔG) is positive.

When EDTA, triethanolamine (TEA), or a thiol (RSH) is used as an electron donor, the following reaction may occur.

$$(HOOCCH_2)_2N(CH_2)_2N(CH_2COOH)_2 + H_2O$$
$$\rightarrow (HOOCCH_2)_2N(CH_2)_2NHCH_2COOH + CO_2 + HCHO + H_2 \quad (17(a))$$

$\Delta G^0 = 80$ kJ mol^{-1} [80,81]

$$N(CH_2CH_2OH)_3 + H_2O \rightarrow NH(CH_2CH_2OH)_2 + CHOCH_2OH + H_2 \quad (17(b))$$

$\Delta G^0 = 120$ kJ mol^{-1} [82]

$$2\ RSH \rightarrow RSSR + H_2 \quad (17(c))$$

$\Delta G^0 = 50$ kJ mol^{-1} [83]

The overall reaction, the light-induced oxidation of electron donor, involves net energy storage and part of the light energy is stored. If the back reaction proceeds by the addition of a suitable catalyst and the stored light energy is taken out as heat, the stored solar energy can be used when needed. With reactions (17(a)) and (17(b)) complex products with three or four components are formed and it is not easy to recover the starting materials through the back reaction. In the case of reaction (17(c)), however, the back reaction proceeds easily. When cystine is used as the disulfide (RSSR), the starting material, cysteine, was produced with palladium catalyst by the hydrogenation of RSSR under mild reaction conditions (at 30°C, hydrogen pressure: 1 atm). After 6 h 60% of RSSR is converted into RSH and no by-product is observed. The conversion of cysteine to cystine and hydrogen leads to storage of 50 kJ mol^{-1} of light energy [83]. The hydrogen production reaction expressed by reaction (17(c)) seems to be suitable for a solar energy storage system. Other electron-donating systems are discussed in Section B(ii).

Photosensitizer

It is almost certain that the excited triplet states of a photosensitizer play an important role for these states have longer lifetimes than the excited singlet state. This is a considerable advantage, since at a given concentration of quencher the number of diffusional encounters between a molecule in an excited state and a quencher molecule will increase when the lifetime of the excited state is extended. More importantly, recent work has established that the separation of photo-redox products is more efficient for a triplet process than for the singlet process. Photophysical properties of excited triplet states for typical photosensitizers are summarized in Table 6. All of the compounds listed in Table 6 have absorption bands in the visible region, and could be used as photosensitizers for solar energy conversion. The lifetimes of the porphyrins are longer than those of ruthenium bipyridine complexes, proflavine, or phthalocyanines. Furthermore zinc porphyrins have a high quantum yield, near unity, for the formation of the triplet excited state. Phthalocyanines absorb light with longer wavelength, and are able to collect up to

TABLE 6

Typical photophysical properties of several photosensitizers for the excited triplet state

Compounds	λ_{max}	τ_T(300 K)(μs)	ϕ_T	E_T(eV)	Ref.
$Ru(bpy)_3^{2+}$	452	0.65	1.0	2.1	114
Proflavine	445	20	–	2.1	109
Zn-$TPPS_4^{4-}$	555	1500	–	–	115
Zn-$TMPyP^{4+}$	560	655	0.9	1.57	105
Zn-TPP	605	1200	0.88	1.59	116,117
H_2-TPP	647	1380	0.82	1.43	118
Chlorophyll-a	661	1000	0.6	1.33	110,119,120
Pc	698	140	0.14	1.24	121–123
Zn-$PcTS^{4-}$	690	245	0.56	1.12	124

λ_{max}, the peak of the absorption band with maximum wavelength; τ_T, lifetime of the excited triplet state; ϕ_T, quantum yield for the formation of the excited triplet state; E_T, the energy of the excited triplet state.

50% of the energy of sunlight [123], but they are apt to aggregate in aqueous solution [124,125]. Porphyrins do not aggregate as easily as phthalocyanines.

The activity of the photosensitizer is very important when the rate-determining step for photoinduced hydrogen evolution is the photoreduction of the electron carrier. When hydrogen evolution is the rate-determining step, however, the efficiency of the reaction depends strongly on the nature of the catalyst used.

Photoinduced hydrogen evolution using bipyridinium salts as electron carriers

When an aqueous solution containing 2-mercaptoethanol, zinc *meso*-tetraphenylporphyrintrisulfonate (Zn-$TPPS_3$) and methylviologen was irradiated, the growth of the reduced methylviologen, with characteristic absorption bands at 395 and 605 nm, is observed. The concentration of reduced methylviologen increases with the irradiation time and tends to reach a constant value. After 60 min irradiation the yield of reduced methylviologen is about 70%. In the course of our studies, Zn-$TPPS_3$ exhibited particularly high activity for this reaction. Many types of bipyridinium salts can replace methylviologen, and some of them are more suitable electron carriers than methylviologen.

When an aqueous solution containing Zn-$TPPS_3$, and an electron carrier (electron carriers are listed in Fig. 17), RSH and hydrogenase was irradiated, hydrogen evolution at a stationary rate, was observed (Fig. 18). It is evident that all the compounds shown in Fig. 17 can serve as electron carriers for photoinduced hydrogen evolution. Hydrogen evolution rates of the systems with compounds A, C and D were much greater than with methylviologen.

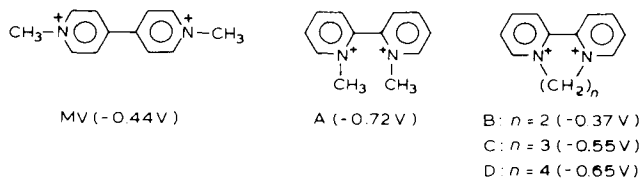

Fig. 17. Electron carriers (figures in parentheses indicate the redox potentials vs. NHE).

In these experiments an excess of hydrogenase was used to make the photoreduction of the electron carriers the rate-determining step for hydrogen evolution.

Sasse et al. [127] observed a wide variation in the ability of diquaternary pyridinium compounds to act as electron-transfer agents in the formation of hydrogen with the system water-$Ru(bpy)_3^{2+}$-EDTA-Pt. The initial rates of hydrogen formation depend primarily on the reduction potential of the electron-transfer agent: as this potential becomes more negative the rate of quenching of $*Ru(bpy)_3^{2+}$ decreases but the hydrogen production step be-

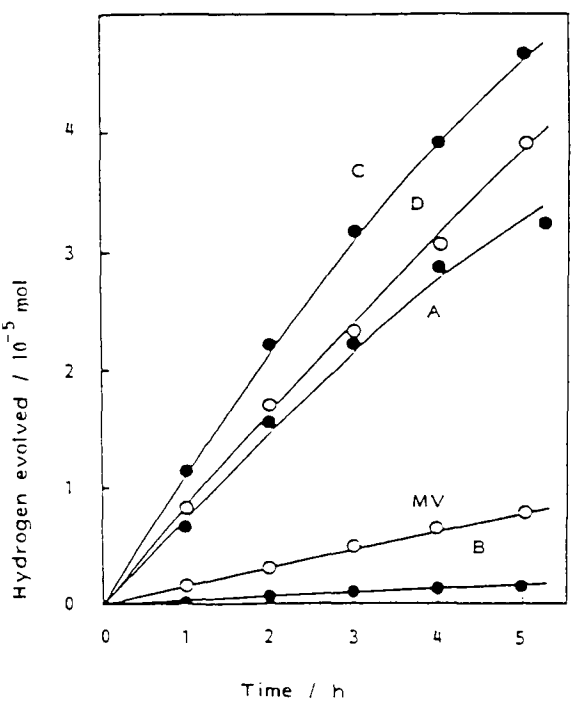

Fig. 18. Time dependence of hydrogen evolution. A sample solution containing RSH (0.2 M), Zn-$TPPS_3$ (7.03×10^{-7} M), bipyridinium salt (1.27×10^{-4} M) and hydrogenase (0.5 ml) is irradiated by visible light at 30°C. Electron carriers labelled as in Fig. 17. Reproduced by permission of the publisher from ref. 126.

comes faster. Consequently, optimum rates of hydrogen formation are associated with diquaternary pyridinium compounds whose reduction potentials lie in a specific range. Since the hydrogen production step is affected by the pH of the system, the optimum range of reduction potential varies with pH. Consequently, this must be taken into account in choosing an electron-transfer agent. The hydrogen yields depend not only on the reduction potential of the electron-transfer agent and the pH of the system but also on the stability of the electron-transfer agent. Catalytic hydrogenation during irradiation is the major pathway for the disappearance of quaternary pyridinium compounds in the system. In practical terms 1,1′,2,2′-tetramethyl-4,4′-bipyridinium diperchlorate and 1,1′,2,2′,6,6′-hexamethyl-4,4′-bipyridinium dichloride are more effective than methylviologen in the production of hydrogen.

Under the reaction conditions, the electron carriers with low redox potentials will be favorably photoreduced. The rate order, however, did not always coincide with the order of the redox potentials of the bipyridinium salts when Zn-$TPPS_3$ was used as a photosensitizer. The rate difference may depend on the efficiency of ion separation after electron transfer from the photoexcited Zn-$TPPS_3$ to the bipyridinium salts. The rates depend strongly on the molecular structure of the bipyridinium salts. Both the rate constants for the following quenching reaction (eqn. 18) and back reaction (eqn. 19) were determined by laser flash photolysis.

$$\text{Zn-TPPS}_3^* + V^{2+} \rightarrow \text{Zn-TPPS}_3^+ + V^+ \tag{18}$$

$$\text{Zn-TPPS}_3^+ + V^+ \rightarrow \text{Zn-TPPS}_3 + V^{2+} \tag{19}$$

where Zn-$TPPS_3^*$ and Zn-$TPPS_3^+$ are photoexcited and oxidized forms of Zn-$TPPS_3$, respectively, and V^{2+} and V^+ denote oxidized and reduced forms of bipyridinium salts respectively.

The triplet state of Zn-$TPPS_3$ has a remarkably long lifetime, 1.6 ms [128]. In the presence of bipyridinium salts, the decay rate of the transient spectrum $\lambda_{max} = 470$ nm (the peak wavelength of the T–T absorption band due to triplet Zn-$TPPS_3$) increases. In a short time period, less than 10 μs after a laser flash, the decay rate follows first order kinetics. From the dependence of lifetime upon various bipyridinium salt concentrations, the quenching rate constants are determined (Table 7). These values are close to that for the diffusion-controlled process.

The quenching efficiency, η_q, of the triplet state of Zn-$TPPS_3$ is expressed as follows

$$\eta_q = k_q[V^{2+}]/(k_0 + k_q[V^{2+}])$$

where $[V^{2+}]$ denotes the concentration of the bipyridinium salt and k_0 is the

TABLE 7

Kinetic parameters obtained from laser flash photolysis of Zn-$TPPS_3$–bipyridinium salt system [126] [a]

	MV	A [b]	B [b]	C [b]	D [b]
k_q(mol^{-1} dm^3 s^{-1})	$(1.5\pm0.3)\times10^{10}$	$(2.5\pm1.8)\times10^{9}$	$(9.9\pm0.9)\times10^{9}$	$(8.7\pm1.3)\times10^{9}$	$(5.3\pm1.2)\times10^{9}$
k_b (relative value)	100	21	38	18	17

[a] The sample solution (6.0 ml) contains Zn-$TPPS_3$ (4.22×10^{-9} mol) and bipyridinium salt (7.62×10^{-7} mol), adjusted with 0.02 M Tris-HCl buffer (pH 7.0). Excitation wavelength, 532 nm.

[b] For electron acceptors, see Fig. 17.

rate constant for the spontaneous deactivation of Zn-$TPPS_3$ triplet state. Under the reaction conditions, since the lifetime is very long (k_0 is very small compared with $k_q[V^{2+}]$), the value of k_q has litttle effect upon η_q.

In longer time periods, greater than 10 μs, the decay of the transient spectrum with $\lambda_{max} = 470$ nm (the peak wavelength of the absorption band due to oxidized Zn-$TPPS_3$ [129]) follows second order kinetics. A typical oscilloscope trace and the second order plot are shown in Fig. 19(a) and Fig. 19(b). From the second order plot (linear plot, OD^{-1} vs. t), the relative back-reaction rate constants (k_b) were determined (Table 7). k_b values depend strongly on the types of bipyridinium salts. When bipyridinium salts

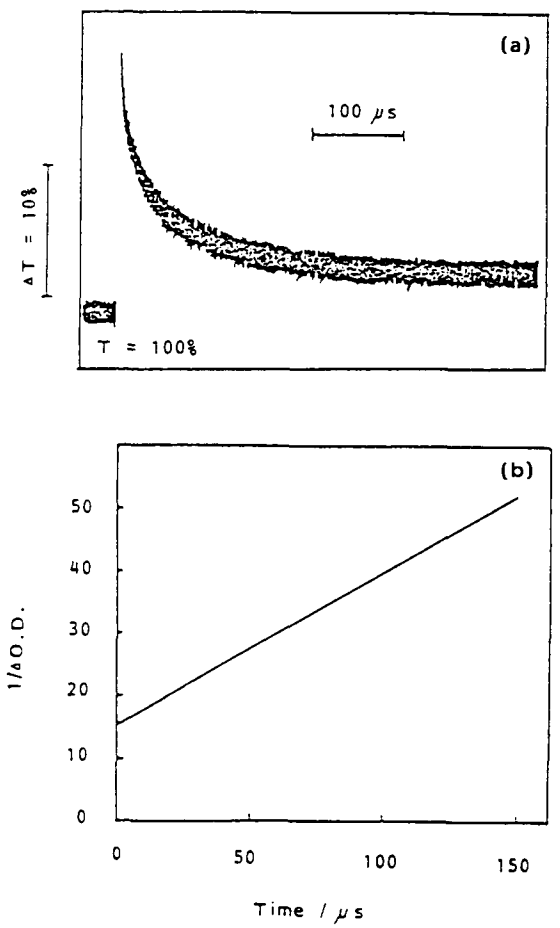

Fig. 19. (a) Oscilloscopic photograph obtained from laser flash photolysis of the aqueous solution (pH 7.0) containing Zn-$TPPS_3$ and methylviologen. (b) Second order plot (OD^{-1} vs. t). Reproduced by permission of the publisher from ref. 129.

having smaller k_b values are used, higher hydrogen evolution rates were observed. As compound B does not have a redox potential high enough to reduce protons and evolve hydrogen, the hydrogen evolution rate is very low, though the k_b value is also relatively small. From these results it is apparent that the back reaction (recombination reaction) plays a role in the photo-induced hydrogen evolution reaction in these systems.

Photoreduction of cytochrome c_3 and hydrogen evolution with hydrogenase [130]

Cytochrome c_3 is a natural electron carrier and the most suitable substrate for hydrogenase, and is expected to be an efficient electron carrier for photoinduced hydrogen evolution. We describe here the photoreduction of cytochrome c_3 by the irradiation of a system containing photosensitizer, cytochrome c_3 and triethanolamine as a reducing agent, and hydrogen evolution catalyzed by hydrogenase.

Hydrogenase (1 ml) was added to 3.51×10^{-9} mol of Zn-TPPS$_3$, 2.30×10^{-9} mol of cytochrome c_3, and 1.0×10^{-3} mol of triethanolamine. The concentration of hydrogenase is not known, but 1.4×10^{-6} mol of hydrogen was generated by the following reaction system; hydrogenase (0.5 cm^3)–methylviologen (2.10×10^{-6} mol)–$Na_2S_2O_4$ (2.30×10^{-5} mol) in 3.0 cm^3 of 0.02 mol dm^{-3} Tris-HCl buffer (pH 7.0). This solution was then irradiated (150 W tungsten lamp) in a Pyrex reaction vessel at 30°C. Light with wavelength shorter than 390 nm was excluded using a Toshiba L-39 filter. A sample of the hydrogen evolved was collected with a sampling valve and analyzed by GLC.

When an aqueous solution containing Zn-TPPS$_3$, cytochrome c_3 and triethanolamine was irradiated, the spectrum of cytochrome c_3 changes (Fig. 20). The spectrum with 419 nm absorption attributed to an oxidized form of cytochrome c_3 decreased and the spectrum with 432 nm absorption appeared. As reduction of cytochrome c_3 with dithionite yielded the same spectrum, the chemical species with 432 nm absorption can be attributed to a reduced form of cytochrome c_3. The concentration of this species increased rapidly at the beginning of the reaction and reached a constant value. After 2 h irradiation almost all of the cytochrome c_3 existed in the reduced form. Aeration of the product leads to immediate reconversion to the starting compound, the oxidized form of cytochrome c_3, without loss.

When 2.80×10^{-8} mol of $Ru(bpy)_3^{2+}$ or 2.36×10^{-8} mol of hematoporphyrin (HmP) was used in place of Zn-TPPS$_3$, no reduction of cytochrome c_3 was observed, though the concentrations of $Ru(bpy)_3^{2+}$ and hematoporphyrin were much higher than that of Zn-TPPS$_3$.

When hydrogenase (1.0 cm^3) was added to the system containing Zn-TPPS$_3$, cytochrome c_3 and triethanolamine and the mixture irradiated with

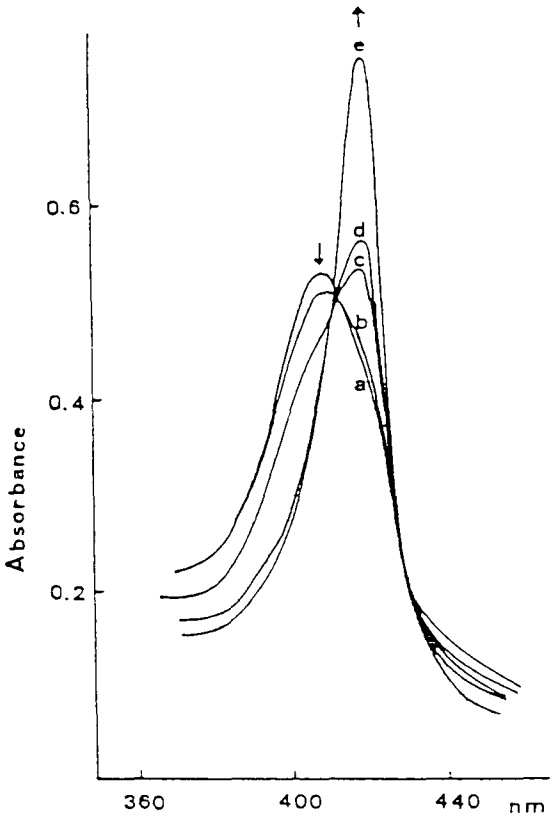

Fig. 20. Change of spectrum with irradiation time. The solution (pH 7.0) containing Zn-TPPS$_3$, cytochrome c_3 and triethanolamine was irradiated for 0 min (a), 6 min (b), 11 min (c), 52 min (d) and 117 min (e). Reproduced by permission of the publisher from ref. 130.

sunlight for 6 h, hydrogen evolution (7.3×10^{-7} mol) was observed. No hydrogen evolution was observed when any component of the system was omitted.

Comparison of hydrogenase and colloidal platinum as a photoinduced hydrogen evolution catalyst

Colloidal platinum is also widely used as a hydrogen evolution catalyst. As the reaction conditions for enzyme catalysis are limited, the replacement of the enzyme, hydrogenase, by artificial heterogeneous or homogeneous catalyst has been undertaken. Hall and his coworkers [131] compared the efficiencies of platinum and hydrogenase and found that both lead to evolution of hydrogen at similar rates (7–9 μmol-H_2 h^{-1} mg-chlorophyll^{-1}) on illumination of isolated chloroplasts with water as the electron source and methylviologen as an electron carrier. The activities, however, should be

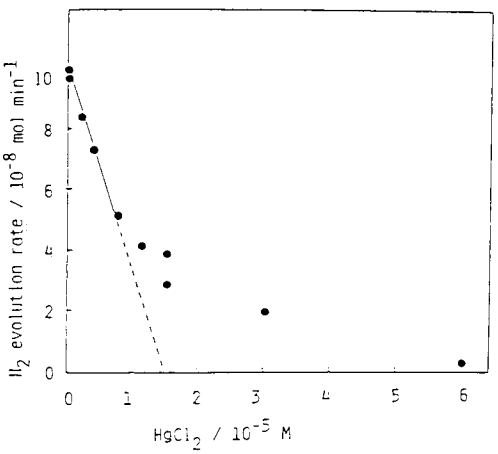

Fig. 21. Effect of mercuric chloride on the hydrogen evolution rate from MV^+ catalyzed by colloidal platinum at pH 7.0. Reproduced by permission of the publisher from ref. 132.

compared by turnover numbers per active site. In this section, an estimation is made of the number of active sites of the colloidal platinum by an inhibition technique. A comparison of the efficiencies and abilities of hydrogenase and colloidal platinum for hydrogen evolution reaction is described.

Figure 21 shows the inhibition effect of $HgCl_2$ on hydrogen evolution rate in the $Na_2S_2O_4$–methylviologen–colloidal platinum system. The initial rate of hydrogen evolution decreases with $HgCl_2$ concentration. Although the rate decreases linearly at low $HgCl_2$ concentrations ($< 1 \times 10^{-5}$ mol dm^{-3}), there are some deviations from the straight line at higher concentrations. Since at low concentration, adsorbed $HgCl_2$ on the colloidal platinum surface may be neglected, the $HgCl_2$ concentration required to inactivate completely the colloidal platinum is calculated by extrapolation as 1.5×10^{-5} mol dm^{-3}. If $HgCl_2$ adsorbs irreversibly, and one molecule of $HgCl_2$ inhibits one active site, the number of active sites on the platinum surface is calculated to be 2.7×10^{15} cm^{-2}. This value corresponds to the number of platinum atoms exposed on the surface. Therefore, the hydrogen evolution per active site (turnover number) is determined to be 3.16×10^{-24} mol min^{-1}. On the other hand, the turnover number per hydrogenase molecule under the same reaction conditions was calculated to be 2.83×10^{-21} mol min^{-1}. As two active sites are involved per hydrogenase molecule (see Section A(i)), the turnover number per active site is 1.41×10^{-21} mol min^{-1}. From these results it is apparent that hydrogenase is about 500 times more active than colloidal platinum.

The time dependences for photoinduced hydrogen evolution by hydro-

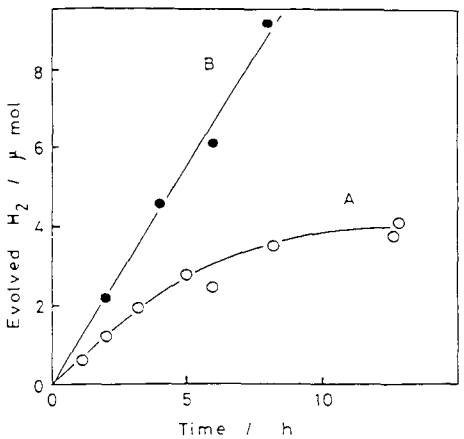

Fig. 22. Time dependence of photoinduced hydrogen evolution with the Zn-$TPPS_3$-methylviologen-RSH system catalyzed by hydrogenase (B) and colloidal platinum (A) at pH 7.0. Reproduced by permission of the publisher from ref. 95.

genase and by colloidal platinum are shown in Fig. 22. In these experiments the concentration of the reduced form of methylviologen was kept constant during the reaction to make sure that the rate-determining step of this reaction was the proton reduction by reduced methylviologen.

In the case of hydrogenase, hydrogen was evolved linearly with time and no deactivation of hydrogenase was observed within 24 h. On the other hand, the hydrogen evolution rate gradually decreased in the case of colloidal platinum (Fig. 22, curve A).

The rate decrease is considered to be caused by colloidal platinum coagulation and/or the decrease of the effective concentration of methylviologen by hydrogenation with the hydrogen produced by colloidal platinum. Johansen et al. and Keller et al. reported that colloidal platinum is active for methylviologen hydrogenation [133,134].

(ii) Other systems for photoinduced hydrogen evolution with hydrogenase

Photoinduced hydrogen evolution in the presence of NADPH as an electron donating agent

Materials such as triethanolamine and EDTA are sacrificial and are consumed when the photoreduction of water is carried out. Unlike these sacrificial reagents, NADPH can be a non-sacrificial electron donor. As shown in eqn. (20), oxidized NADPH (NADP, or D_{ox}) is easily photoreduced in the presence of grana, obtained from green plants.

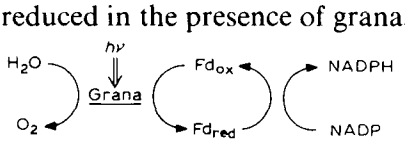

(20)

By combining reactions (15) and (20), the splitting of water into hydrogen and oxygen is accomplished. Therefore, it is important to know whether NADPH can serve as an electron donor in the photoinduced hydrogen evolution system as shown in eqn. (15).

When Zn-$TPPS_3$ is used for the photoreduction of methylviologen using NADPH, formation of MV^+ is observed as shown in Fig. 23(c). When HmP dissolved by cetyltrimethylammonium bromide (CTAB) or Triton X-100 is used in place of Zn-$TPPS_3$, the reduction of methylviologen proceeds with a much higher reduction rate compared with the [NADPH–Zn–$TPPS_3$–MV^{2+}] system as shown in Fig. 23(a) and (b). When HmP is dissolved by sodium dodecylsulphate (SDS), reduction of methylviologen does not proceed.

The differences in reaction activity between CTAB, Triton X-100 and SDS systems are related to the difference in the surface charge of the micelles [136]. The reaction activity also depends on the type of viologen used. Though the methylviologen reduction rate is greater than that of propylsulfonate viologen (PVS) in the [NADPH–HmP/Triton X-100–viologen] system, the PVS reduction rate is greater than that of methylviologen in the [NADPH–HmP/Triton X-100–viologen] system.

In every micellar system, ^{3}HmP is quenched not only by methylviologen and PVS, but also by NADPH; quenching rate constants are shown in Table 8. In the [HmP/Triton X-100–MV^{2+}] system, formation of MV^+ corresponding to the decay of ^{3}HmP is observed and the quenching rate constant

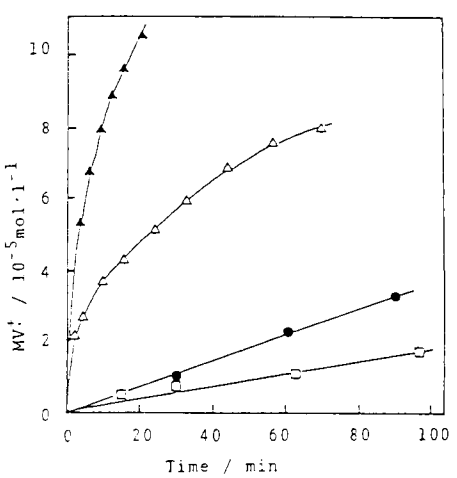

Fig. 23. Time dependence of MV^+ upon steady-state irradiation of aqueous solution (6.0 ml) containing MV^{2+} (2.44×10^{-5} mol), NADPH (2.16×10^{-5} mol), and Hm (CTAB, 4.28×10^{-7} mol: ▲ (a)), Hm (Triton X-100, 5.04×10^{-7} mol: △ (b)), Hm (SDS, 4.26×10^{-7} mol: ●), or Zn-$TPPS_3$ (3.63×10^{-7} mol: □ (c)) [135].

TABLE 8

Quenching rate constants of ^{3}HmP by several quenchers in micellar solution (pH 7.0) [135]

Quencher	k_q ($mol^{-1}\,dm^3\,s^{-1}$)	
	HmP/CTAB	HmP/Triton X-100
MV^{2+}	6.7×10^5	9.3×10^7
PVS	7.2×10^7	8.9×10^6
NADPH	6.3×10^5	3.7×10^5

HmP,hematoporphyrin.

by NADPH is about two orders of magnitude smaller than that by viologens. In the [HmP/Triton X-100–viologen] system, the oxidative quenching is dominant. In the [HmP/CTAB–viologen] system, the ^{3}HmP quenching rate constant by PVS is about two orders of magnitude larger than that by methylviologen. Under steady state irradiation the reduction rate, however, in the [HmP/CTAB–MV^{2+}] system is greater than that in the [HmP/CTAB–PVS] system. The differences in the reduction rate may be explained by eqns. (21–24).

$$[^3HmP]_m + MV^{2+} \xrightarrow{k_q} [HmP^+\cdots MV^+]_m \begin{cases} \xrightarrow{k_1} [HmP]_m + MV^{2+} \\ \xrightarrow{k_2} [HmP^+]_m + MV^+ \end{cases} \quad (21)$$

$$[^3HmP]_m + PVS \xrightarrow{k_q'} [Hmp^+\cdots PVS^-]_m \begin{cases} \xrightarrow{k_1'} [HmP]_m + PVS \\ \xrightarrow{k_2'} [HmP^+]_m + PVS^- \end{cases} \quad (22)$$

$$[HmP^+]_m + MV^+ \xrightarrow{k_b} [HmP]_m + MV^{2+} \quad (23)$$

$$[HmP^+]_m + PVS^- \xrightarrow{k_b'} [HmP]_m + PVS \quad (24)$$

(Subscript m denotes micelle.)

Equations (21) and (22) express quenching reactions of ^{3}HmP by viologen and charge separation or back electron transfer within the solvent cage. Equations (23) and (24) denote the back electron-transfer reactions between the separated ion pairs.

Though k_q is smaller than k_q' as listed in Table 8, the charge separation in the [HmP/CTAB–MV^{2+}] system may be much easier than that in the [HmP/CTAB–PVS] system. In the former system, since HmP^+, MV^+ and the micelle surface are all positively charged, the electrostatic repulsion may enhance charge separation and may suppress the back reaction between the separated ion pairs (eqn. 23). In the latter system, since the charges of HmP^+ and PVS^- are different in sign, the back electron transfer in the solvent cage (k_1' in eqn. 22) may be more favorable than the charge

separation (k_2' in eqn. 22). As PVS^- and the micelle surface also differ in sign, the back reaction between the separated ion pairs (eqn. 24) may be faster than that in the [HmP/CTAB–MV^{2+}] system. Therefore, the reduction rate of viologens in the [NADPH–HmP/CTAB–MV^{2+}] system under steady state irradiation may be greater than that in the [NADPH–HmP/CTAB–PVS] system, though the quenching rate constant in the former is smaller than that in the latter.

In the [HmP/Triton X-100–viologen] system, ^{3}HmP was quenched by MV^{2+} with the formation of the transient absorption at 605 nm, which was attributed to the absorption of MV^+. In the [HmP/Triton X-100–PVS] system, the same results were observed. These results suggest that the photoreduction of viologens in the [NADPH–HmP/Triton X-100–viologen] system under steady state irradiation proceeds predominantly via oxidative quenching of ^{3}HmP by viologens.

In the [NADPH–HmP/SDS–MV^{2+}] system, photoreduction of MV^{2+} was not observed even though ^{3}HmP was quenched. This may be caused by the surface charge on the micelle. Since the surface charges of the SDS micelle and MV^+ differ in sign, the efficiency of charge separation may decrease and the possibility of the back reaction between the separated ion pairs may increase.

When hydrogenase was added to the system containing HmP, methylviologen and NADPH, hydrogen evolution was observed. The amount of hydrogen evolved for 1.5, 3.0, and 6.0 h irradiation was 0.19, 0.34, and 0.45 μmol, respectively.

Photoinduced cleavage of water with the chloroplast–ferredoxin–hydrogenase system

Green plants split water under irradiation by sunlight. The brief reaction mechanism of the green plant photosystem is shown in Fig. 24. Green plants extract electrons by oxidising water with the aid of light energy and the electrons are transported into the Calvin cycles through ferredoxin. The arrows in Fig. 24 show the electron flow. By the addition of hydrogenase to

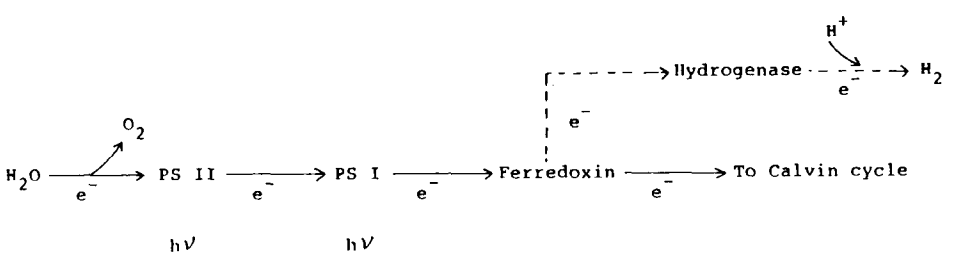

Fig. 24. Diagram of electron flows in photosystem.

extract electrons from the ferredoxin, the electrons are made to flow in the direction shown by the dotted arrow and hydrogen evolves through the reduction of protons. Photoinduced hydrogen evolution is reported through the irradiation of a system containing chloroplast–ferredoxin–hydrogenase. The main results are summarized in Table 9. The amount of hydrogen evolved per mg-chloroplast is about 10 μmol. Rao et al. [131] reported 188 μmol of hydrogen evolution per 2 h irradiation.

In each system, however, the hydrogen evolution rate decreases with irradiation time, and it is difficult to obtain hydrogen continuously for a long time. The cause of the decrease is the simultaneous evolution of oxygen, which is a strong inhibitor for hydrogenase. To obtain hydrogen over a long period it is necessary to remove oxygen. One method is to consume oxygen by addition of glucose and glucose oxidase. Another method is to develop a hydrogenase which is unaffected by oxygen. Kamen et al. [139] found that the hydrogenase from *Clostridium pasteurianum* when fixed on glass beads, is more stable towards oxygen.

To avoid enzyme deactivation by oxygen, Greenbaum et al. [140] used a flow system comprising a cylinder of compressed carrier gas (either helium or nitrogen) which continually purges the reaction cuvettes and electrolysis cell. They have measured the simultaneous photoproduction of hydrogen and oxygen in marine green algae. *Chlamydomonas* species (clone f-9), for example, has a steady state rate of hydrogen and oxygen production during irradiation with a stoichiometric ratio near 2 : 1.

Yagi has developed an enzymic electric cell to separate hydrogenase-catalyzed hydrogen-producing system (cathode reaction) from the electron-donating system (anode reaction) in order to protect hydrogenase from the by-products of electron-donating reactions [141].

D. CONCLUSIONS

In this review, we have described hydrogenase catalysis and the extensive research concerning photoinduced hydrogen evolution with hydrogenase as

TABLE 9

Photoinduced hydrogen evolution with the chloroplast–ferredoxin–hydrogenase system

Hydrogen evolved	Chloroplast	Irradiation time	References
0.25 μmol	0.8 mg	15 min	137
10μmol	1 mg	1 h	138
60–70 μmol	1 mg	7–8 h	139
30–50 μmol	1 mg	1 h	131
(Maximum 188 μmol/mg chloroplast/2 h)			

an application of this enzyme. Information about the active sites of hydrogenase is accumulating and the reaction mechanisms are becoming clearer. Model studies are especially useful for the elucidation of the mechanisms (Section B).

Hydrogenase contains at the least Fe_4S_4-type clusters. If we assume that a Fe_4S_4-cluster is the site of hydrogen activation or production, then an explanation for the function of other clusters is needed. One probable function lies in the transfer of electrons to and from the active site. Thus an external carrier would transfer electrons to or from these accessory sites and the electron would then be passed intramolecularly to the hydrogenase site at which, when combined with protons, hydrogen is evolved (Fig. 15).

Nickel in hydrogenase may be another accessory site and may be essential for the catalytic activity of hydrogenase. However, hydrogenases from some bacteria do not contain nickel. Elucidation of the role played by nickel is now in progress.

Hydrogenase is still the most active and selective photoinduced hydrogen evolution catalyst (no by-product is formed). Since enzymes are not ideally suited for long-term use, replacement of hydrogenase by homogeneous or heterogeneous catalysts is needed. Colloidal platinum serves as a hydrogen evolution catalyst, but the activity, per active site is very low compared with hydrogenase. Moreover colloidal platinum is active for the hydrogenation of electron carriers, such as methylviologen. Colloidal platinum is apt to coagulate and the activity decreases with reaction time. We do not have an ideal hydrogen evolution catalyst, and the development of a new catalyst and new system is a subject for a future study. Further fundamental studies of the present excellent catalyst, hydrogenase, are needed.

ACKNOWLEDGEMENT

I express my appreciation to Professor Tominaga Keii and Professor Yoshio Ono for their stimulating and helpful discussions. I also would like to thank members of the laboratories of Professor Keii and Professor Ono for their help with the hydrogenase work.

REFERENCES

1 H. Gust, Bacteriol. Rev., 18 (1954) 43.
2 L.E. Mortenson and J.-S. Chen, Microbial Iron Metabolism, Academic Press, New York, 1974, p. 231.
3 M.W.W. Adams, L.E. Mortenson and J.-S. Chen, Biochim. Biophys. Acta, 594 (1981) 105.
4 P.H. Gitlitz and A.I. Krasna, Biochemistry, 14 (1975) 2561.
5 T. Kakuno, N.O. Kaplan and M.D. Kamen, Proc. Natl. Acad. Sci., U.S.A., 74 (1977) 861.

6 H. van Heerikhuizen, S.P.J. Albracht, B. tenBtrink, L. Evers-van Twist and E.C. Slater, Hydrogenases: Their Catalytic Activity, Structure and Function, E. Goltze KG, Gottingen, 1978, p. 151.
7 M.W.W. Adams and D.O. Hall, Arch. Biochem. Biophys., 195 (1979) 288.
8 R.N.F. Thorneley, Biochim. Biophys. Acta, 333 (1974) 487.
9 K. Schneider and H.G. Schlegel, Biochim. Biophys. Acta, 452 (1976) 66.
10 K. Schneider, R. Cammack, H.G. Schlegel and D.O. Hall, Biochim. Biophys. Acta, 578 (1979) 445.
11 M.W.W. Adams and D.O. Hall, Biochem. J., 183 (1979) 11.
12 J.-S. Chen and L.E. Mortenson, Biochim. Biophys. Acta, 371 (1974) 283.
13 J.-S. Chen, L.E. Mortenson and G. Palmer, Iron and Copper Proteins, Plenum Press, New York, 1976, p. 68.
14 W.O. Gillum, L.E. Mortenson, J.-S. Chen and R.H. Holm, J. Am. Chem. Soc., 99 (1977) 584.
15 T. Yagi, A. Endo and K. Tsuji, Hydrogenases: Their Catalytic Activity, Structure and Function, E. Goltze KG, Gottingen, 1978, p. 109.
16 I. Okura, K. Nakamura and T. Keii, J. Mol. Catal., 4 (1978) 453.
17 I. Okura, K. Nakamura and S. Nakamura, J. Mol. Catal., 6 (1979) 307.
18 I. Okura, K. Nakamura and S. Nakamura, J. Mol. Catal., 6 (1979) 311.
19 T. Yagi, J. Biochem., 68 (1970) 649.
20 H.M. Van der Westen, S.G. Mayhew and C. Veeger, FEBS Lett., 86 (1978) 122.
21 S.G. Mayhew, C. van Dijk and H.M. Van der Westen, Hydrogenases: Their Catalytic Activity, Structure and Function, E. Goltze KG, Gottingen, 1978, p. 125.
22 A.D. Kidman, B.A.C. Ackrell and R.S. Asato, Biochim. Biophys. Acta, 159 (1968) 185.
23 G.R. Bell, J.P. Lee, H.D. Peck, Jr. and J. LeGall, Biochemie, 60 (1978) 315.
24 H. Hartman and A.I. Krasna, Biochim. Biophys. Acta, 92 (1964) 52.
25 P.H. Gitlita and A.I. Krasna, Biochemistry, 14 (1975) 2561.
26 G. Nakos and L.E. Mortenson, Biochemistry, 10 (1971) 2442.
27 L. Que, Jr., R.H. Holm and L.E. Mortenson, J. Am. Chem. Soc., 97 (1975) 463.
28 B.A. Averill, J.R. Bale and W.H. Orme-Johnson, J. Am. Chem. Soc., 100 (1978) 3034.
29 I. Okura, K. Nakamura and S. Nakamura, J. Mol. Catal., 6 (1979) 299.
30 D.L. Erbes, R.H. Burris and W.H. Orme-Johnson, Proc. Natl. Acad. Sci., U.S.A., 72 (1975) 4795.
31 E.C. Hatchikian, M. Bruschi and J. LeGall, Biochem. Biophys. Res. Commun., 82 (1978) 451.
32 M. Teixeira, I. Moura, A.V. Xavier, D.V. DerVartanian, J. LeGall, H.D. Peck, Jr., B.H. Huynh and J.J.G. Moura, Eur. J. Biochem., 130 (1983) 481.
33 R. Cammack, D. Patil, R. Aguirre and E.C. Hatchikian, FEBS Lett., 142 (1982) 289.
34 H.-J. Kruger, B.H. Huynh, P.O. Ljungdahl, A.V. Xavier, D.V. DerVartanian, I. Moura, H.D. Peck, Jr., M. Teixeira, J.J.G. Moura and J. LeGall, J. Biol. Chem., 257 (1982) 14620.
35 M.V. Lalla-Maharagh, D.O. Hall, R. Cammack, K.K. Rao and J. LeGall, Biochem. J., 209 (1983) 445.
36 S.P.J. Albracht, E.G. Graft and R.K. Thauer, FEBS Lett., 140 (1982) 311.
37 N. Kojima, J. Fox, R. Hausinger, L. Daniels, W.H. Orme-Johnson and C. Walsh, Proc. Natl. Acad. Sci., U.S.A., 80 (1983) 378.
38 S.P.J. Albracht, K.Y. Albrecht-Elmer, D.J.M. Schmedding and E.C. Slater, Biochim. Biophys. Acta, 681 (1982) 330.
39 C.G. Friedrich, K. Schneider and B. Friedrich, J. Bacteriol., 52 (1982) 42.

40 J.J.G. Moura, M. Teixeira, I. Moura, A.V. Xavier and J. LeGall, J. Mol. Catal., 23 (1984) 303.
41 B.H. Huynh, M.H. Czechowski, H.-J. Kruger, D.V. DerVartanian, H.D. Peck, Jr. and J. LeGall, Proc. Natl. Acad. Sci., U.S.A., 81 (1984) 3728.
42 W.B. Lovenberg, B. Buchanan and J.C. Rabinowitz, J. Biol. Chem., 238 (1963) 3899.
43 R. Malkin and J.C. Rabinowitz, Biochem. Biophys. Res. Commun., 23 (1966) 822.
44 J. Hong and J.C. Rabinowitz, Biochem. Biophys. Res. Commun., 29 (1967) 246.
45 E. Bayer, D. Josef, P. Krauss, H. Hagenmaier, A. Roder and A. Trebst, Biochim. Biophys. Acta, 143 (1967) 435.
46 V. Suzuki, Biochemistry, 6 (1967) 1335.
47 J.C.M. Tsibris, M.J. Namtvedt and I.C. Gunsalus, Biochem. Biophys. Res. Commun., 30 (1968) 323.
48 K.K. Rao, R. Cammack, D.O. Hall and C.E. Johnson, Biochem. J., 122 (1971) 257.
49 C.L. Thompson, C.E. Johnson, D.P.E. Dickson, R. Cammack, D.O. Hall, U. Weser and K.K. Rao, Biochem. J., 139 (1974) 97.
50 L.E. Mortenson and J.-S. Chen, Microbial Production and Utilization of Gases, E. Goltze KG, Gottingen, 1978, p. 57.
51 D.L. Erbes and R.H. Burris, Biochim. Biophys. Acta, 525 (1978) 45.
52 B.R. Glick, W.G. Martin, J.J. Giroux and R.E. Williams, Can. J. Biochem., 57 (1979) 1093.
53 C. van Dijk, S.G. Mayhew, H.J. Grande and C. Veeger, Eur. J. Biochem., 102 (1980) 317.
54 I. Okura, N. Nakamura and S. Nakamura, J. Inorg. Biochem., 14 (1981) 155.
55 T. Yagi, M. Goto, K. Nakao, K. Kimura and H. Inokuchi, J. Biochem., 78 (1975) 443.
56 T. Yagi, K. Kimura, H. Daidoji, F. Sakai, S. Tamura and H. Inokuchi, J. Biochem., 79 (1976) 661.
57 I. Okura, T. Kita and S. Aono, J. Mol. Catal., 24 (1984) 1.
58 I. Okura, S. Nakamura and K. Nakamura, J. Mol. Catal., 5 (1979) 315.
59 K. Tanno and G.N. Schrauzer, J. Am. Chem. Soc., 97 (1975) 5404.
60 G.N. Schrauzer and T.D. Guth, J. Am. Chem. Soc., 98 (1976) 3508.
61 G. Henrici-Olive and S. Olive, J. Mol. Catal., 1 (1975/76) 121.
62 E.G. Chepaikin and M.L. Khidekel, J. Mol. Catal., 4 (1978) 103.
63 K. Suzuki and T. Kimura, Biochem. Biophys. Res. Commun., 28 (1967) 514.
64 K.W. Lovenberg and K. McCarthy, Biochem. Biophys. Res. Commun., 30 (1968) 453.
65 I. Okura, S. Nakamura and K. Nakamura, J. Mol. Catal., 6 (1979) 71.
66 I. Okura, S. Nakamura and M. Kobayashi, Bull. Chem. Soc. Jpn., 54 (1981) 3794.
67 T. Herskovitz, B.A. Averill, R.H. Holm, J.A. Ibers, W.H. Phillips and J.F. Weiher, Proc. Natl. Acad. Sci., U.S.A., 69 (1972) 2437.
68 J.J. Mayerle, S.E. Denmark, B.V. DePamphilis, J.A. Ibers and R.H. Holm, J. Am. Chem. Soc., 97 (1975) 1032.
69 B.A. Averill, T. Herskovitz, R.H. Holm and J.A. Ibers, J. Am. Chem. Soc., 95 (1973) 3523.
70 J.J. Mayerle, R.B. Frankel, R.H. Holm, J.A. Ibers, W.D. Phillips and J.F. Weiher, Proc. Natl. Acad. Sci., U.S.A., 70 (1973) 2429.
71 M.A. Borik, L. Que, Jr. and R.H. Holm, J. Am. Chem. Soc., 96 (1974) 285.
72 B.V. DePemphilis, B.A. Averill, T. Herskovitz, L. Que, Jr. and R.H. Holm, J. Am. Chem. Soc., 96 (1974) 4159.
73 L. Que, Jr., M.A. Borik, J.A. Ibers and R.H. Holm, J. Am. Chem. Soc., 96 (1974) 4168.
74 E. Bayer, D. Josef, P. Krauss, H. Hagenmaier, A. Roder and A. Trebst, Biochim. Biophys. Acta, 143 (1967) 435.

75 K. Suzuki, Biochemistry, 6 (1967) 1335.
76 M.W.W. Adams, S.G. Reeves, D.O. Hall, G. Christou, B. Ridge and H.N. Rydon, Biochem. Biophys. Res. Commun., 79 (1977) 1184.
77 J.R. Darwent, P. Douglas, A. Harriman, G. Porter and M.-C. Richoux, Coord. Chem. Rev., 44 (1982) 83, and references therein.
78 J. Kiwi, K. Kalyanasundaram and M. Grätzel, Struct. Bonding, 49 (1982) 37, and references therein.
79 K.I. Zamaraev and V.N. Parmon, Russ. Chem. Rev., 52 (1983) 818, and references therein.
80 M. Calvin, Energy Res., 3 (1979) 73.
81 A. Harriman and A. Mills, J. Chem. Soc., Faraday Trans. 2, 77 (1981) 2111.
82 M. Kirch, J.-M. Lehn and J.P. Sauvage, Helv. Chim. Acta, 62 (1979) 1345.
83 A. Harriman: Energy Resources through Photochemistry and Catalysis, Academic Press, New York, 1983.
84 J.-M. Lehn and J.P. Sauvage, Nouv. J. Chim., 1 (1977) 449.
85 K. Kalyanasundaram, J. Kiwi and M. Grätzel, Helv. Chim. Acta, 61 (1978) 2720.
86 A. Moradpour, E. Amouyal, P. Keller and H. Kagan, Nouv. J. Chim., 2 (1978) 547.
87 J. Kiwi and M. Grätzel, Nature, 281 (1979) 657.
88 D. Miller and G. McLendon, Inorg. Chem., 20 (1981) 950.
89 M. Maestri and D. Sandrini, Nouv. J. Chim., 5 (1981) 637.
90 M. Gohn and N. Getoff, Z. Naturforsch., Teil A, 34 (1979) 1135.
91 I. Okura, S. Nakamura, N. Kim-Thuan and K. Nakamura, J. Mol. Catal., 6 (1979) 261.
92 V. Balzani, L. Moggi, M.F. Manfrin, F. Bolletta and M. Gleria, Science, 189 (1975) 852.
93 K. Kalyanasundaram and M. Grätzel, J. Chem. Soc., Chem. Commun., (1979) 1137.
94 I. Okura and N. Kim-Thuan, J. Mol. Catal., 5 (1979) 311.
95 I. Okura and N. Kim-Thuan, J. Chem. Soc., Chem. Commun., (1980) 84.
96 I. Okura and N. Kim-Thuan, J. Chem. Soc., Faraday Trans. 1, 76 (1980) 2209.
97 I. Okura and N. Kim-Thuan, J. Mol. Catal., 6 (1979) 227.
98 I. Okura, M. Takeuchi and N. Kim-Thuan, Chem. Lett., (1980) 765.
99 I. Okura, M. Takeuchi and N. Kim-Thuan, Photochem. Photobiol., 33 (1981) 413.
100 I. Tabushi and A. Yazaki, J. Org. Chem., 46 (1981) 1899.
101 G. McLendon and D.S. Miller, J. Chem. Soc., Chem. Commun., (1980) 533.
102 K. Kalyanasundaram and M. Grätzel, Helv. Chim. Acta, 63 (1980) 478.
103 A. Harriman, G. Porter and M.-C. Richoux, J. Chem. Soc., Faraday Trans. 2, 77 (1981) 1939.
104 A. Harriman, G. Porter and M.-C. Richoux, J. Chem. Soc., Faraday Trans. 2, 77 (1981) 833.
105 R. Ballardini, A. Juris, G. Varani and V. Balzani, Nouv. J. Chim., 4 (1980) 563.
106 A.I. Krasna, Photochem. Photobiol., 29 (1979) 267.
107 K. Kalyanasundaram and D. Dung, J. Phys. Chem., 84 (1980) 2551.
108 K. Kalyanasundaram and G. Porter, Proc. R. Soc. London, Ser. A, 369 (1978) 29.
109 M. Grätzel and J. Kiwi, J. Phys. Chem., 84 (1980) 1503.
110 J.R. Benemann, J.A. Berenson, N.O. Kaplan and M.D. Kaman, Proc. Natl. Acad. Sci., USA, 70 (1973) 2317.
111 A.A. Krasnovskii, V.V. Nikandrov, G.P. Brin, I.P. Gogotov and V.P. Oschepkov, Dokl. Akad. Nauk, SSSR, 225 (1975) 711.
112 V. Balzani, F. Bolletta, M.T. Gandolpi and M. Maestri, Topics Curr. Chem., 75 (1978) 1.
113 M.-C. Richoux and A. Harriman, J. Chem. Soc., Faraday Trans. 1, 78 (1982) 1873.
114 A. Harriman, J. Chem. Soc., Faraday Trans. 2, 77 (1981) 1281.

115 G.P. Gurinovich and B.M. Dzhagarov, Izv. Akad. Nauk, SSSR, 37 (1973) 383.
116 A. Harriman, J. Chem. Soc., Faraday Trans. 1, 76 (1980) 1978.
117 G. Seeley, Photochem. Photobiol., 27 (1978) 639.
118 P.G. Bowers and G. Porter, Proc. R. Soc. London, Ser. A, 296 (1967) 435.
119 M.J. Whally, J. Chem. Soc., (1961) 866.
120 P.S. Vincett, E.M. Voight and K.E. Riechhoff, J. Chem. Phys., 55 (1971) 4131.
121 J.G. Villar and L. Lindquist, C.R. Acad. Sci., Ser. B, 264 (1967) 1807.
122 A. Harriman, G. Porter and M.-C. Richoux, J. Chem. Soc., Faraday Trans. 2, 76 (1980) 1618.
123 M.-C. Richoux, Photogeneration of Hydrogen, Academic Press, New York, 1982, p. 39.
124 A. Harriman and M.-C. Richoux, J. Photochem., 14 (1980) 253.
125 J.R. Darwent, J. Chem. Soc., Chem. Commun., (1980) 805.
126 I. Okura, N. Kaji, S. Aono, T. Kita and A. Yamada, Inorg. Chem., 24 (1985) 451.
127 A. Launikonis, J.W. Loder, A.W.-H. Mau, W.H.F. Sasse, L.A. Summers and D. Wells, Aust. J. Chem., 35 (1982) 1341.
128 I. Okura, S. Aono, M. Hoshino and A. Yamada, Bull. Chem. Soc. Jpn., 58 (1985) 749.
129 I. Okura, S. Aono, M. Hoshino and A. Yamada, Inorg. Chim. Acta, 86 (1984) L55.
130 I. Okura, M. Takeuchi, S. Kusunoki and S. Aono, Chem. Lett., (1982) 187.
131 K.K. Rao, I.N. Gogotov and D.O. Hall, Biochimie, 60 (1978) 291.
132 I. Okura, S. Kusunoki, N. Kim-Thuan and M. Kobayashi, J. Chem. Soc., Chem. Comm., (1981) 56.
133 O. Johansen, A. Launikonis, A.W.-H. Mau and W.H.F. Sasse, Aust. J. Chem., 33 (1980) 1643.
134 P. Keller and A. Moradpour, J. Am. Chem. Soc., 102 (1980) 7193.
135 I. Okura and S. Aono, Photochem. Photobiol., in press.
136 K. Takuma, M. Kajiwara and T. Matsuo, Chem. Lett., (1977) 1199.
137 K.K. Rao, L. Rosa and D.O. Hall, Biochem. Biophys. Res. Commun., 68 (1976) 21.
138 I. Fry and G. Papageorgiou, Z. Naturforsch., Teil C, 32 (1977) 110.
139 D.A. Lappi, F.E. Stoizenbach, N.A. Kaplan and M.D. Kamen, Biochem. Biophys. Res. Commun., 69 (1976) 878.
140 E. Greenbaum, R.R.L. Gullard and W.G. Gunda, Photochem. Photobiol., 37 (1983) 649.
141 T. Yagi, Biological Solar Energy Conversion, Academic Press, New York, 1977, p. 61.